Icarus 211 (2011) 347–365

Contents lists available at ScienceDirect

Icarus

journal homepage: www.elsevier.com/locate/icarus

Preservation of Late Amazonian Mars ice and water-related deposits in a unique crater environment in Noachis Terra: Age relationships between lobate debris tongues and gullies

Gareth A. Morgan [a,*], James W. Head [a], David R. Marchant [b]

[a] Department of Geological Sciences, Brown University, Providence, RI 02912, USA
[b] Department of Earth Sciences, Boston University, Boston, MA 02215, USA

ARTICLE INFO

Article history:
Received 2 April 2010
Revised 2 August 2010
Accepted 7 August 2010
Available online 13 August 2010

Keywords:
Mars, Climate
Mars, Surface
Planetary dynamics

ABSTRACT

The Amazonian period of Mars has been described as static, cold, and dry. Recent analysis of high-resolution imagery of equatorial and mid-latitude regions has revealed an array of young landforms produced in association with ice and liquid water; because near-surface ice in these regions is currently unstable, these ice-and-water-related landforms suggest one or more episodes of martian climate change during the Amazonian. Here we report on the origin and evolution of valley systems within a degraded crater in Noachis Terra, Asimov Crater. The valleys have produced a unique environment in which to study the geomorphic signals of Amazonian climate change. New high-resolution images reveal Hesperian-aged layered basalt with distinctive columnar jointing capping interior crater fill and providing debris, via mass wasting, for the surrounding annular valleys. The occurrence of steep slopes (>20°), relatively narrow (sheltered) valleys, and a source of debris have provided favorable conditions for the preservation of shallow-ice deposits. Detailed mapping reveals morphological evidence for viscous ice flow, in the form of several lobate debris tongues (LDT). Superimposed on LDT are a series of fresh-appearing gullies, with typical alcove, channel, and fan morphologies. The shift from ice-rich viscous-flow formation to gully erosion is best explained as a shift in martian climate, from one compatible with excess snowfall and flow of ice-rich deposits, to one consistent with minor snow and gully formation. Available dating suggests that the climate transition occurred >8 Ma, prior to the formation of other small-scale ice-rich flow features identified elsewhere on Mars that have been interpreted to have formed during the most recent phases of high obliquity. Taken together, these older deposits suggest that multiple climatic shifts have occurred over the last tens of millions of years of martian history.

1. Introduction

The presence of extensive fluvial features (e.g., widespread dendritic valley networks) on ancient martian terrain suggests that a relatively 'warm and wet' climate was prevalent early in the planet's history (Carr, 1996). Such conditions provide a strong contrast to the hyper-arid, extremely cold climate (characterized by temperatures and pressures largely below the triple point of H_2O; Hecht, 2002) that is thought to have persisted throughout the Amazonian, up to the present (e.g., Bibring et al., 2006). Within the context of a general Amazonian polar desert-like environment (Baker, 2001), the hydrological system is horizontally layered and most water resides in a buried global cryosphere and in the polar caps, with minute amounts in the atmosphere. In contrast to the Noachian, there is little evidence of liquid water substantially shaping the surface. Marchant and Head (2007) and Krevslasky et al. (2008), however, have emphasized that local microenvironments may support short-term melting under optimal conditions. Furthermore, Laskar et al. (2004) have documented extreme variations in insolation caused by the substantial range of spin-axis/orbital parameter variations of Mars. These results show that even in the hyper-arid cold desert environment of Amazonian Mars, ice can be transported from polar reservoirs to the mid-latitudes (Head et al., 2006a,b) and to the equatorial regions (Head and Marchant, 2003; Shean et al., 2005, 2007a; Forget et al., 2006; Kadish et al., 2008). The placement of high-resolution instruments into Mars orbit has made it possible to observe the effects of such recent climate change and candidate melting conditions. For example, the presence of geologically young (<1 Myr), small-scale (~1 km in length) gullies (Malin and Edgett, 2000a), argues for the localized temporal stability of liquid water at the surface within the most recent period of the Amazonian. Therefore, understanding the detailed nature of Amazonian climate history is an

* Corresponding author. Present address: Center for Earth and Planetary Studies, National Air and Space Museum, Smithsonian Institute, Washington, DC 20560, USA.
E-mail address: MorganGA@si.edu (G.A. Morgan).

0019-1035/$ - see front matter © 2010 Elsevier Inc. All rights reserved.
doi:10.1016/j.icarus.2010.08.004

important goal and is essential for assessing the potential for life to have existed on the planet over its recent history.

The thin atmosphere and low temperatures that are thought to have persisted on Mars throughout the Amazonian (Carr, 1996) mean that water-related landforms (regardless of whether in the solid or liquid phase) can be important indicators of the presence of specific environmental conditions. For example, the presence of fluvial landforms, however limited in distribution and scale, can indicate the presence of climatic conditions conducive to surface melting (i.e. surface temperatures above 273 K, assuming the absence of salts, which can enable melting point depression). The presence of deposits indicative of glaciers, without evidence for basal or surface melting, signals the presence of climatic conditions permitting sufficient accumulation of snow and ice to cause cold-based ice flow (i.e. glaciers that are frozen to their bed and flow through internal deformation rather than basal sliding). The combination of glacial landforms and meltwater might signal conditions favoring wet-based glaciation. Finally, superposition and overprinting of landforms produced by cold-based ice with those of a fluvial origin point to initial glacial conditions *followed* by melting conditions (e.g., Milliken et al., 2003; Head et al., 2008).

In summary, many landforms are produced within a narrow range of conditions and thus can be extremely sensitive indicators of local climate. The linkage of climatically sensitive surface processes and resultant landforms, e.g., climatic geomorphology, is highly dependent on both the spatial scales of the landscapes being studied and the temporal scales over which the landforms are generated. For climatic geomorphology, the assumptions are either that (1) the landforms observed are in equilibrium with prevailing climate conditions (see also Chorley et al. (1985) for more discussion); or (2) for large-scale landforms and landscapes that have evolved over long periods of time and experienced multiple climatic transitions, the distinctive elements inherited from past conditions are still preserved and recognizable in the morphologic record. As an example of the latter, we highlight the combined imprints of both ancient fluvial incision and modern glaciation that are still preserved within the Antarctic Dry Valleys (Sugden et al., 1995; Jamieson et al., 2008). Likewise, on Mars the fretted valleys and associated alcoves along the northern dichotomy boundary of Mars show evidence for initial alteration by liquid water during the Early Hesperian (Irwin et al., 2004) followed by subsequent Amazonian glaciation (e.g., Head et al., 2006b).

Here we report on geomorphological investigations of Asimov Crater located in Noachis Terra at 46°S, 5°E (Figs. 1–3), a site chosen because of its unique mid-latitude setting and its distinctive topographic configuration that displays an unusually wide range of insolation conditions. Within the site we have identified a multitude of distinctive ice-and-water-related landforms of various scales, including lobate debris tongues and gullies. Through the morphological analyses of these features, and investigations of their relative age and stratigraphy, we reconstruct and interpret changes in local climatic conditions during the Late Amazonian. We then place this analysis within the context of larger-scale morphological investigations conducted elsewhere on Mars (e.g., Mustard et al., 2001; Milliken et al., 2003; Head et al., 2006a,b; Morgan et al., 2009).

2. Data sets and analysis

The identification of landforms made use of all available image data sets. The study area was initially chosen because of its unusual setting and the extensive available imagery, including full coverage of Context Imager (CTX) images (8 m/pixel) and High Resolution Stereo Camera (HRSC) images (18 m/pixel), in addition to 16 HiRISE images (0.3 m/pixel) and 73 Mars Orbital Camera (MOC) narrow angle images (1.5–12 m/pixel). The investigation was conducted using a Geographical Information System (GIS) database comprised of the visible image data sets co-registered and overlain on digital terrain models (DTMs). The topographic data was derived from both 128 pixel/degree gridded Mars Orbiter Laser Altimeter (MOLA) data and Mars Express HRSC stereo data (200 m/pixel) derived from HRSC orbit 1932_0000. ESRI's ArcMap (9.2) provided the GIS platform, which in addition to data set management was also used to produce slope maps and topographic

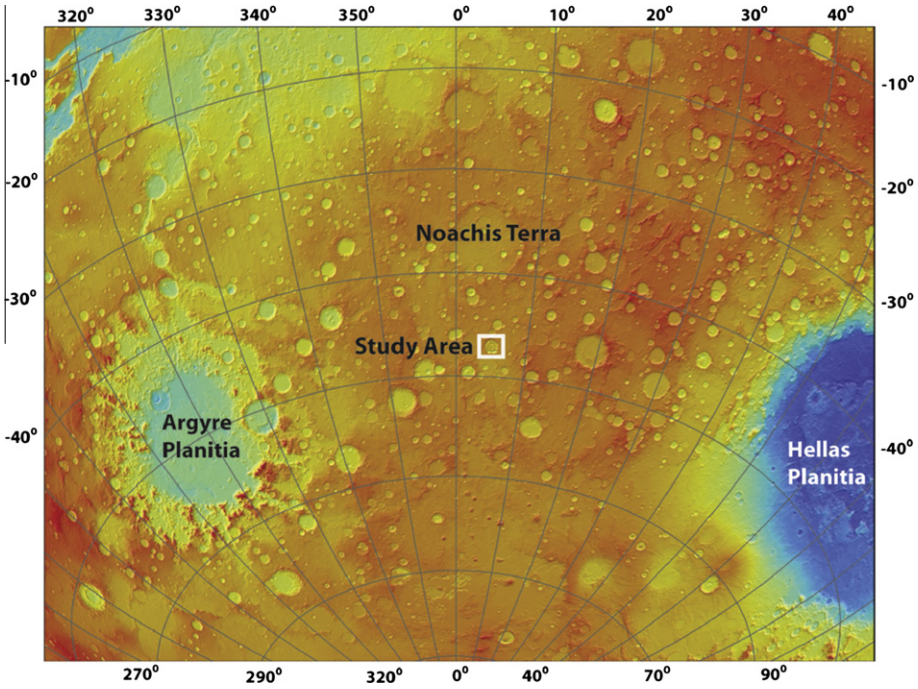

Fig. 1. Regional setting of the Asimov Crater study area on Mars. MOLA shaded relief overlain on MOLA gridded data. Red is high, blue is low. (For interpretation of the references to color in this figure legend, the reader is referred to the web version of this article.)

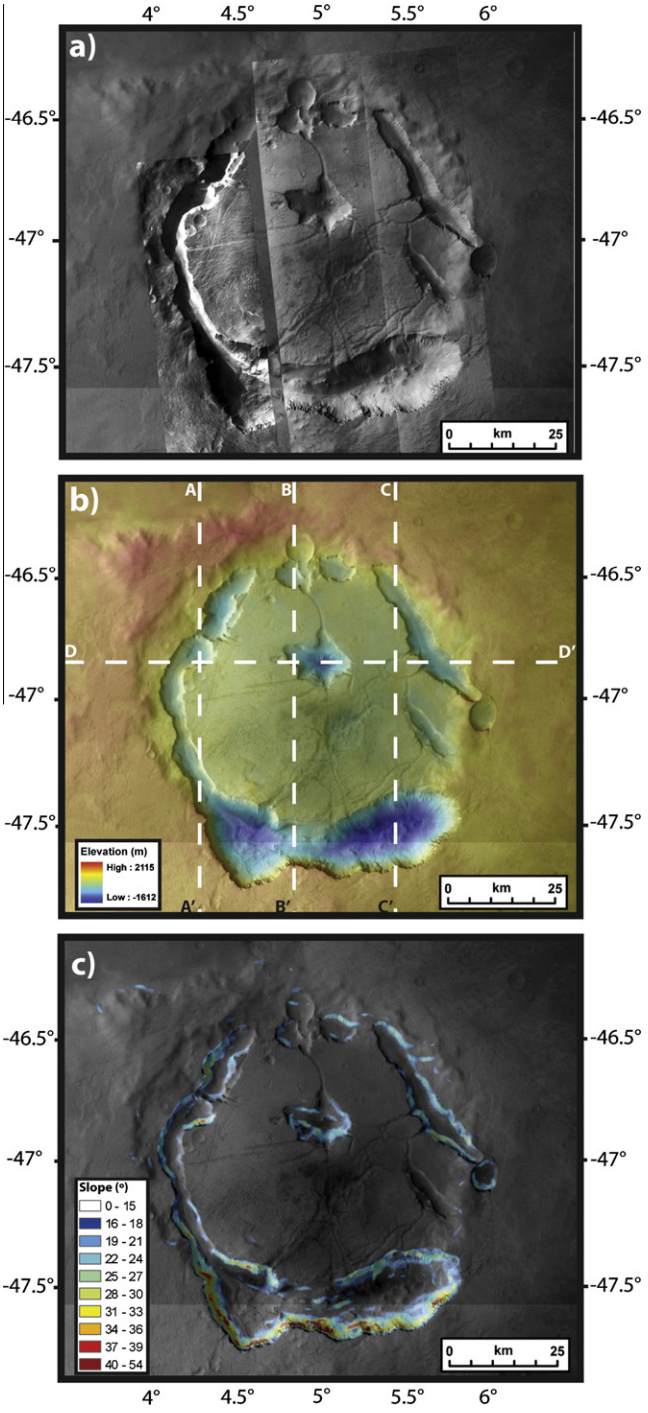

Fig. 2. Asimov Crater in Noachis Terra located at 46°S, 5°E. (a) The interior of the crater contains an annulus of valley systems and an off-center depression. CTX data over HRSC image: h1932_0000. (b) DTM of the study region. The degraded rim of the crater can be seen in the topographic data to the northwest. The deepest valley is 2000 m below the average surface elevation of the crater floor. The dashed white lines are the location of topographic transects in Fig. 4. DTM derived from HRSC orbit: h1932_0000. (c) Slope map of slopes >15° in the study area. Slope measurements derived from HRSC orbit: h1932_0000.

profiles from the HRSC DTMs. In the areas where detailed measurements of slopes were required, individual MOLA points were extracted to provide the most accurate account of the topography. The GIS software also enabled crater diameter surveys to be conducted and size–frequency distribution plots to be compiled in order to estimate the age of surfaces. Thermal infrared data from daytime and nighttime THEMIS infrared images (band 9, 100 m/pixel) were used to characterize the thermal inertia of the surface, which in turn provides a proxy for the physical properties of the surface (such as grain sizes).

3. Geological setting of the Asimov Crater study region

Research was focused within the 80-km diameter Asimov impact crater located within the heavily cratered plains of Noachis Terra to the west of Hellas (Fig. 1). This region of Mars has been mapped within the Southern Highlands hilly and cratered unit (Nhc) and is interpreted to be the oldest extensively exposed surface of the planet (Scott and Carr, 1978). The crater has no identifiable ejecta deposit and its remaining rim is both discontinuous and heavy degraded (Figs. 2 and 3), suggesting that it is Noachian in age. The floor of the crater is highly modified and filled and consists of a relatively flat unit that forms a surface ~1500 m below the highest portion of the crater rim crest (~900 m below the surrounding terrain outside of the crater, Fig. 4). Depths for a fresh crater of this scale are empirically found to be >3 km according to the depth (h) to diameter (D) relationship compiled by Garvin et al. (2003):

$$h = 0.36D^{0.49} \quad (1)$$

This suggests that the crater has been significantly in-filled since its formation in the Noachian. The crater interior is unusual in that there is an annulus of disconnected valleys adjacent to the interior flanks of the crater wall (Figs. 2 and 3). These valley systems extend for a collective length of over 200 km, and their widths range from 3 km in the eastern basin interior to over 18 km at their widest in the south (Figs. 2 and 4). The valleys range from 200 to 2000 m below the current crater floor (1700–3500 m below the crater rim crest, see Fig. 4), and thus the floors of the valleys might represent a portion of the original crater floor, prior to it being filled with material. An irregular ~20 km wide depression is also present north of the center of the crater (Figs. 2–4). The depression is connected to surrounding valley complexes by a network of radial ~1 km wide, shallow (~20 m deep) troughs.

A fine-grained deposit is draped along the majority of surfaces within the study area and is interpreted to be related to the latitude-dependant mantle that has been observed poleward of 30° latitude on Mars (Kreslavsky and Head, 2000; Mustard et al., 2001). This mantling unit has been attributed to an atmospherically derived layer of dust-rich ice which formed during the most recent Mars 'ice age' when obliquity values were higher than today (Head et al., 2003). Although smooth in appearance relative to all other surfaces within the crater, the mantle unit exhibits several different textures including ~10 m wide isolated pits and extended regions of cuspate depressions (Fig. 7). Similar dissected morphology has also been observed in the global mantle unit in the latitude range of 30–60° (Mustard et al., 2001; Milliken et al., 2003). This has been attributed to sublimation of water ice within the mantle caused by the current instability of near-surface ice-rich material at these latitudes (Mustard et al., 2001; Mellon and Jakosky, 1995).

In the highest-resolution image data sets (MOC and HiRISE) a discrete layer is observed in section along the upper, steeper portions of the valley slopes where it is exposed from beneath the upper mantle layer (Figs. 5–7). This unit is also apparent in the THEMIS nighttime infrared data where it correlates with a layer of higher nighttime temperatures relative to the slopes directly below (Fig. 8). This indicates that it corresponds to a material with a higher thermal inertia value, and likely represents a rock outcrop similar to others identified on Mars with THEMIS (Christensen, 2003). The layer appears to be actively eroding, providing a source of scree and large boulders (>5 m) that are present across all slopes directly below outcrops (Figs. 5 and 7). Boulder tracks, 1 m in

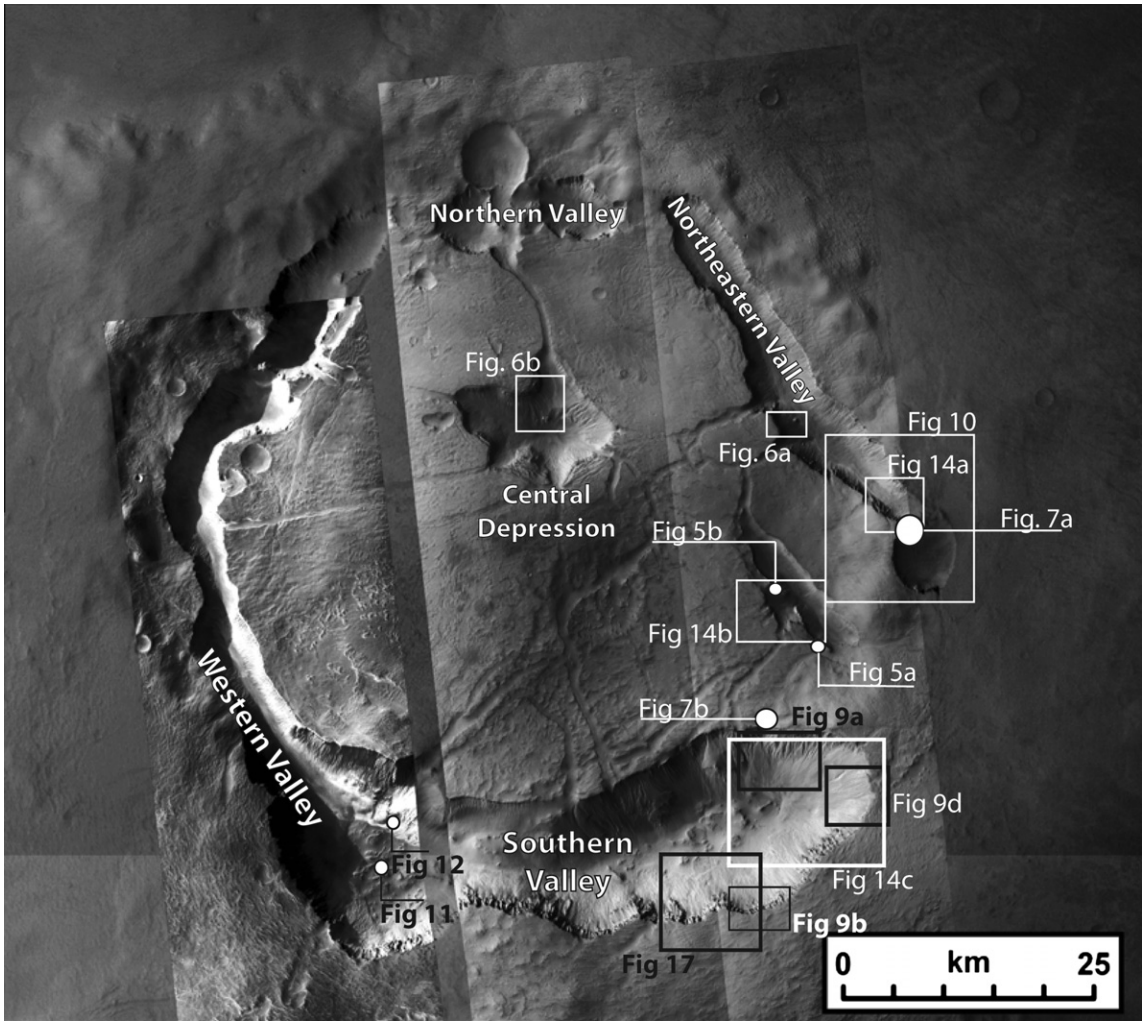

Fig. 3. Location of figures and names of valleys within Asimov Crater. CTX data over HRSC image: h1932_0000.

width, are visible in the highest-resolution images, suggesting that the erosion has been recent. In some sections, the rock layer forms an overhang, indicating that it is more resistant than lower portions of the slopes (Fig. 6).

In areas that have HiRISE coverage it is possible to observe and study exposed outcrops of the rock layer in detail (Figs. 5–7). Prominent and pervasive polygonal fracture patterns ~10 m wide are visible along the surface of the rock layer outcrops, suggesting that erosion has exploited the surface expression of the vertical rock structure (Fig. 5a). In regions where a vertical perspective of the outcrops is possible, columns of rock tens of meters tall with polygonal cross sections form the rock face (Fig. 5b). The boulders on the slopes directly below the rock layers have similar diameters to the polygonal fractures and most likely represent columns of rock that have toppled from the cliff face (Fig. 5). The structure of the rock layer closely resembles the columnar jointing present in terrestrial lava flows (Spry, 1962; Long and Wood, 1986). This type of columnar jointing is caused by contractional stresses during the cooling of the upper thermal boundary layer of a lava flow (Spry, 1962; Long and Wood, 1986; Degraff et al., 1989; Grossenbacher and McDuffie, 1995). Hence, the rock layer most likely represents a lava unit that was emplaced in the interior of the crater and possibly also forms the surrounding plains.

Information on the nature of the lava flow units and their cooling history can be obtained from column scale and height. Cooling from the top and bottom of the flow creates thermal boundary layers that upon solidification form columnar structures known as colonnades (Spry, 1962). Large-diameter columns are favored by slower cooling and large flows, with a slow cooling rate permitting viscous dissipation to act over a larger region (Grossenbacher and McDuffie, 1995). Toramaru and Matsumoto (2004) found that basaltic column area is inversely proportional to cooling rate. The height or thickness of columns is also related to flow thickness. The upper colonnade (well-formed basaltic columns) typically occurs in the upper third of a flow, the lower colonnade in the lower third, with entablature (irregular to hackly columns) forming the middle third (Long and Wood, 1986). On the basis of the width of the columns (~10 m) and the geometry of the colonnade (columns >30 m tall) we interpret the colonnades to represent the top of a lava flow that was at least 100 m in thickness (and may have been much thicker) and experienced very slow cooling to produce the very wide columns. Some workers interpret entablature in cooling terrestrial flows to form when the flow top is flooded by rainwater, inducing rapid cooling, convection and more irregular structure, with colonnades being favored by slower cooling by conductive heat transfer in the absence of water (Degraff et al., 1989). The tall colonnade observed on Mars in this example may be favored by the hyper-arid environment and the lack of rainwater. The apparent slow cooling and large flow thickness of this unit is consistent with the mode of emplacement of the Late Noachian

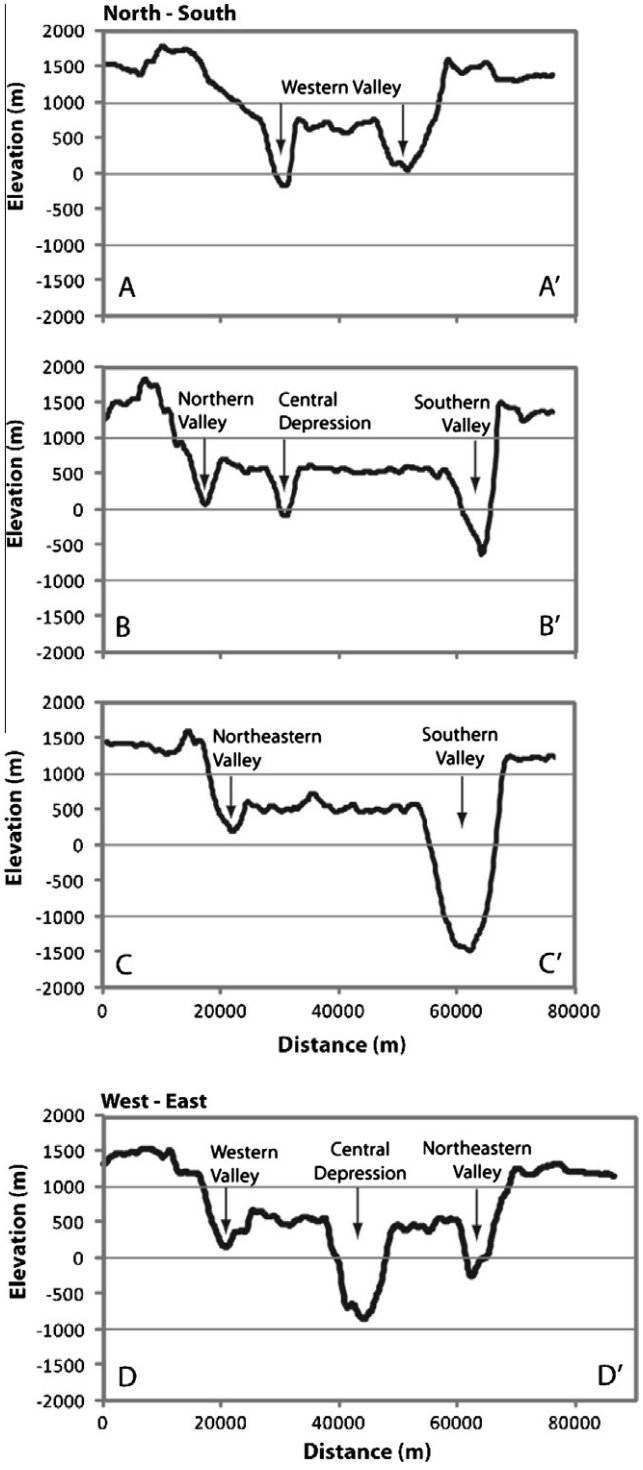

Fig. 4. Topographic profiles across the Asimov Crater. The interior of the crater has a relatively consistent elevation of ~500 m; the floors of the valleys and the central depression are 300–2000 m below this elevation, suggesting that the crater is filled with ~2 km of material. Topography derived from HRSC DTM orbit: h1932_0000.

and Hesperian ridged plains in the region, thought to be emplaced in a flood lava mode (Peterson, 1977), fed by very large dikes (Head et al., 2006c).

In addition to the downslope movement of material from rock fall, large-scale slumping also appears to have occurred (Fig. 6). Kilometer-long arcuate fractures are present on the surface of the lava unit scarp where it is exposed at the top of the valley flanks, suggesting the development of rotational slump fractures (Fig. 6). Isolated exposures of the rock unit are found downslope of the main lava unit and are interpreted to represent slump blocks that detached from the slopes above (Fig. 6). As a result of the mass wasting operating along the valley walls, a layer of colluvium has developed below the outcropping rock layer. Therefore, it is not possible to determine unequivocally the full thickness of the lava unit. On the basis of the height of the scarp outcrop seen in Figs. 5 and 6, and our initial estimates derived from colonnade thickness, we conclude that the thickness of the upper flow unit to be of the order of >100 m; assuming uniform emplacement, this would account for about 5% of the total estimated volume of fill in the crater interior (depth of ~2 km). The pre-lava crater fill in this region may be related to Noachian-aged fine-grained deposits as described for elsewhere on Mars by Cabrol and Grin (1999).

The abrupt change in slope associated with the surface of the steep-cliffed lava units near the top of the valleys has made it possible to observe the mantle in cross section as it approaches the cliff edges (Fig. 7). This also permits estimates of the mantle thickness and internal structure. Measurements were made throughout the study area where the mantle could be clearly observed, and provided an average mantle thickness of ~20 m, consistent with other mantle thickness measurements in lowland regions (Morgenstern et al., 2007). In some places along cliff faces, the occurrence of distinct bands of boulders associated with the top of the underlying lava flow unit (Fig. 7) suggests that the mantle does not completely cover the lava flow, and may have been partially removed, possibly as a result of the mass wasting described above.

The formation of the deep concentric valleys clearly postdates the formation of the crater, the deposition of crater fill, and the emplacement of lava (dating from the Noachian and Hesperian), but predates the emplacement of the Late Amazonian latitude-dependent mantle. The large-scale morphology and structure of the crater provide a geologic context for the environment in which the Amazonian landforms have developed. The formation of the valleys within the crater has been previously studied by several authors and has been attributed to the concentrated excavation of fill material along the interior walls of the crater (Schultz and Glicken, 1979; Malin and Edgett, 2000b). Malin and Edgett (2000b) acknowledge the absence of any obvious removal mechanisms to account for the loss of the crater fill material, but suggest that it may have been possible under a different climatic regime than is currently present. Alternatively Schultz and Glicken (1979) draw attention to similar valley depressions within younger craters elsewhere in Noachis Terra and suggest that a regional episode of endogenic activity (igneous intrusions) could have induced the collapse and removal of portions of the crater fill through the thawing of ground ice. Our observations indicate that a thick layer of lava (>100 m) was emplaced over a lower layer of less-resistant crater fill material (~2 km thick). The extent to which the top-most rock layers overhang the lower slopes argues against the lower portions of the crater fill being lava-flow-like in nature and instead suggests a weaker lithology, possibly sedimentary in origin. The estimated ~2 km thickness of this weaker-fill unit is consistent with sedimentary units identified within Noachian craters elsewhere on Mars (Cabrol and Grin, 1999). The occurrence of radial fractures in the crater center may be a response to the load imposed by the emplacement of thick lava units over relatively weak sedimentary units. If volatiles were present within the sedimentary unit, as has been suggested for similar deposits in other martian craters (e.g. Schultz and Lutz, 1988; Fassett and Head, 2007), the release of these volatiles could have accounted for the loss of material required to form the valleys systems and central depression as suggested by Schultz and Glicken (1979). Slumping, and rock falls along the edge of the valley flanks would over time cause a widening of the valleys, and appears to be continuing into the

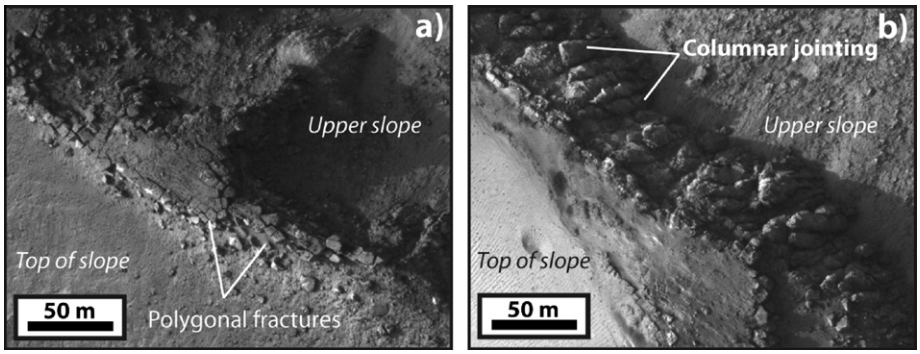

Fig. 5. Exposed columnar jointing along the edge of the rock layer that caps the valley walls. (a) Polygonal fractures 10 m in diameter are present within the surface of the rock layer close to the top of the valley slopes. (b) Perspective view of 30 m high structural columns within the rock layer. The columns have the same diameter as the polygonal fractures seen in (a). This structure is similar to columnar jointing that forms in terrestrial basaltic flows as a result of thermal contraction during cooling. This suggests that the rock layer was formed by a lava flow on top of the crater fill. HiRISE images: PSP_003603_1325 (a), PSP_003669_1325 (b).

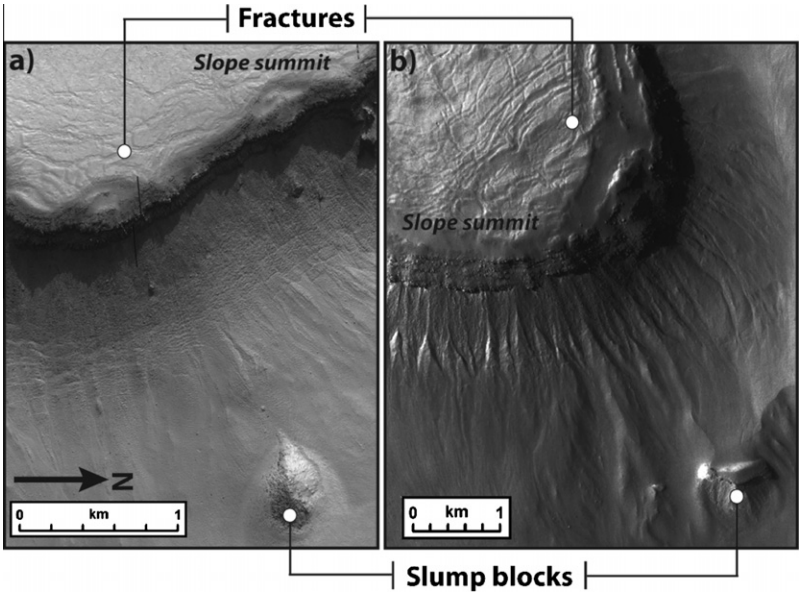

Fig. 6. Evidence for mass wasting in the form of slumping along the slopes of the valleys. Boulders within the slump blocks suggest that the blocks originated from the rock layer at the top of the slopes. Arcuate fractures along the surfaces above the valley slopes imply that extension has occurred, which may contribute to further detachment of the steep scarps. (a) Western slope of the northeastern valley complex. HiRISE image: PSP_003814_1325. (b) Northern slope within the central depression. CTX image: P05_003102_1327. See Fig. 3 for location.

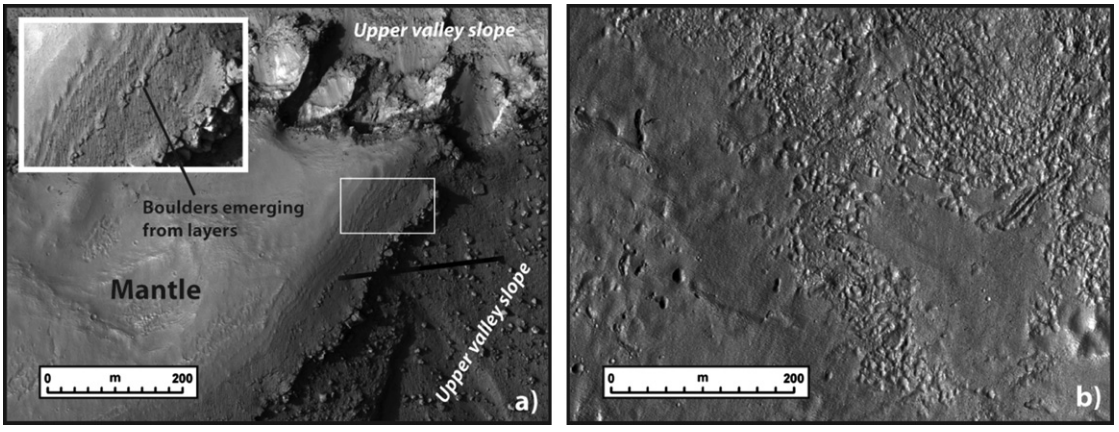

Fig. 7. Morphology of the latitude-dependent mantle within Asimov Crater. (a) Along the top of the plateau edge the mantle forms a distinct layer above the coherent lava flow rock layer. The abrupt change in slope along the edge of the rock layer provides a perspective view of the mantle, which in some areas appears to be several tens of meters thick and consists of multiple layers. In some places, the occurrence of boulders emerging from the layers suggests that these are regions where the mantle is relatively thin (near the cliff edge) and the structure of the underlying rock layers shows through. (b) Example of degradational textures along the surface of the mantle, including isolated pits and shallow cuspate depressions. These features have been attributed to the loss of ice through sublimation (Mustard et al., 2001). HiRISE images: PSP_003880_1325 (a) and PSP_003603_1325 (b).

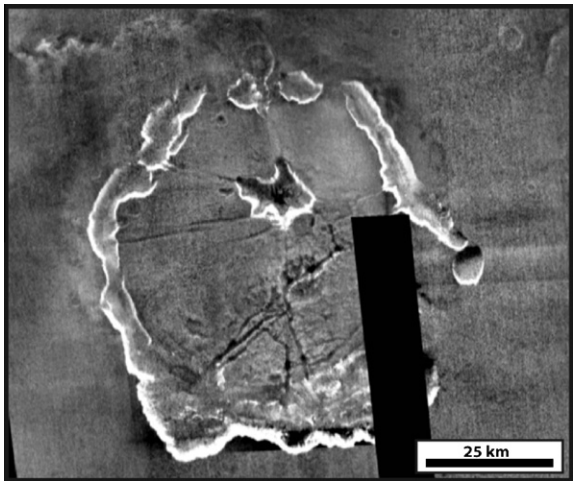

Fig. 8. Mosaic of THEMIS infrared nighttime images covering Asimov Crater. The relatively high temperatures along the top of the valleys (bright pixels) are correlated with a discrete rock layer (see Fig. 5) and are thus likely caused by the high thermal inertia of the rock layer (and associated boulders) relative to loose sediments and dust that cover the rest of the surface.

present. These observations provide a geological and topographic context for the environments in which the late Amazonian climate-related landforms have formed.

4. Geomorphic evidence for liquid water and ice

In the following section, we describe the assemblage of ice-related landforms that we have identified within the valleys and the central depression of Asimov Crater (Fig. 3). These features are compared to ice-related landforms previously identified elsewhere on Mars in order to assess the climatic and geomorphologic processes under which they formed. We have endeavored to determine both relative an absolute ages for the landforms so that the temporal relationships between the different landform types can be established.

4.1. Gullies

The discovery of gullies on Mars has significant implications for the record of Amazonian climate because of the apparent role of liquid water in their formation and because of their very youthful nature (Malin and Edgett, 2000a). Gullies are typically ~1–2 km long and are distributed poleward of ~30° in both hemispheres, along steep slopes (>10°) within crater interiors, valleys walls, and the flanks of mesas (Malin and Edgett, 2000a; Dickson et al., 2007). The latitude dependence of gully distribution strongly suggests a climatic cause and the involvement of a volatile component in their formation. Liquid water provides the most plausible erosional agent and is consistent with the occurrence of fine-scale fluvial features (McEwen et al., 2007), including dendritic tributaries (Malin and Edgett, 2000a), levees (Malin and Edgett, 2000a) and the striking similarity between the martian gullies and terrestrial analogs formed by ephemeral runoff in polar regions (e.g. Lee et al., 2001; Costard et al., 2002; Head et al., 2007; Morgan et al., 2008).

Models of gully formation require an explanation of how pressure/temperature conditions optimal for melting and water flow can be achieved on the surface of Mars (albeit briefly) during the Late Amazonian. Initial models invoked the rapid release of groundwater discharge from perched aquifers (Malin and Edgett, 2000a; Heldmann and Mellon, 2004). This mechanism was favored as melting of near-surface ice deposits was considered difficult under martian conditions (Mellon and Phillips, 2001). Further detailed investigations into the current/recent metastability of liquid water on the surface of Mars generated alternative explanations, including melting of atmospherically deposited sources of water (Hecht, 2002; Costard et al., 2002; Christensen, 2003; Dickson et al., 2007; Williams et al., 2009). Many of the models propose that gullies formed during periods of higher obliquity when H_2O ice is redistributed from the poles to the mid-latitudes (Costard et al., 2002; Milliken et al., 2003; Christensen, 2003; Dickson et al., 2007; Head et al., 2003; Morgan et al., 2010). This has included the results of recent detailed modeling of martian snowpacks that has shown surficial melting can occur under the insolation conditions created at high obliquity (Williams et al., 2009). The release of water and CO_2 ice from the poles via sublimation under high obliquity conditions would have also increased the surface atmospheric-pressure (Kieffer and Zent, 1992) and water vapor content of the atmosphere (Mellon and Jakosky, 1995), and thus further encouraged gully development. Recent repeated HiRISE observations have shown the appearance of fresh gully deposits within some gully systems (Dundas et al., 2010; Diniega et al., 2010). CO_2 driving processes and dry granular flow have been suggested as possible formation mechanisms for these deposits, though it is unclear whether these processes can drive a significant portion of gully erosion (Dundas et al., 2010) or have been responsible for the complex fluvial features (McEwen et al., 2007) observed within the most dendritic gully systems. Overall, the study of gullies has the potential to be used to identify microclimate zones where ice-rich deposits were able to accumulate and melt during recent martian history, and thus provide a proxy for recent climate change.

4.1.1. Location and morphology

Gullies are present along every slope within the valley systems and the central depression; their morphology, however, is highly dependent on slope aspect (Fig. 9). Morgan et al. (2010) previously examined this difference in gully morphology. They determined that variations in insolation geometry over time could account for the morphological differences as a result of top-down heating and melting of surface snow; their model is consistent with other gully studies that suggest an atmospherically deposited water source (Hecht, 2002; Costard et al., 2002; Christensen, 2003; Head et al., 2007; Dickson et al., 2007). Here, and in later sections, we expand upon the Morgan et al. (2010) work and assess gully relationships with other ice-related landforms.

The poleward-facing gullies within the study area (Fig. 9a) are highly developed and heavily incised into the slopes of the valley walls. The gullies typically consist of multiple tributaries which originate in alcoves within the outcropping cap-rock unit at the top of the slope and merge down slope to form single ~100 m wide channels that open up into fan deposits. At MOC and HiRISE resolution (sub-meter) it is possible to identify individual, 5-m wide sinuous channels incised within major channels (Fig. 9c); these nested channels exhibit streamlined islands and potential terraces, similar to those identified in gullies elsewhere on Mars (McEwen et al., 2007). The gullies on north (equatorward-facing) slopes (Fig. 9b) display morphologic and scale differences relative to the poleward-facing gullies; these gullies originate in ~500 m wide amphitheater-shaped alcoves that are eroded into the cap-rock unit. Multiple, relatively straight channels originate from the apex at the bottom of the alcoves and extend for 500–1000 m until they open up into fan deposits (Fig. 9b). The equator-facing gully channels lack the dendritic system of tributaries present in the poleward-facing gullies and are significantly less incised into the valley wall. The occurrence of gullies on isolated slopes along the narrow walls (300 m wide) that divide the heads of the

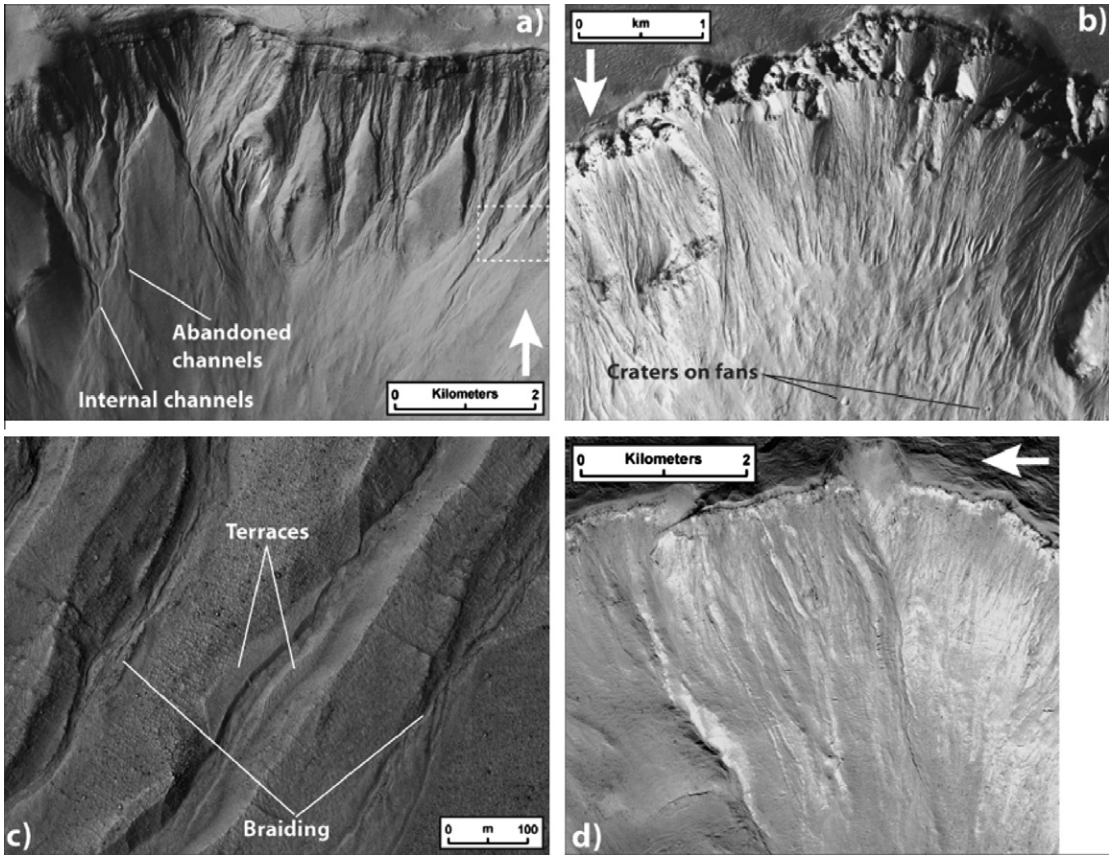

Fig. 9. Aspect dependence of the morphology of gullies within Asimov Crater. (a) Gullies on pole-facing slopes are highly incised and display dendritic tributaries that merge into single ~100 m wide channels. (b) Gullies on equator-facing slopes originate from cuspate, ~500 m wide alcoves cut into the upper portion of the slopes. Multiple, relatively straight, 50 m wide channels emerge from the apex of the alcoves. (c) High-resolution image of pole-facing gully channels that display fluvial features, including small ~5 m-wide channels that are present within the larger channel systems (see box in (a) for location). (d) Gullies on west-facing slopes are also well incised, but are not as densely eroded into the slopes as the pole facing gullies are and do not display tributaries. (a) and (b) CTX: P07_003880_1327. (c) and (d) HiRISE image: PSP_004091_1325.

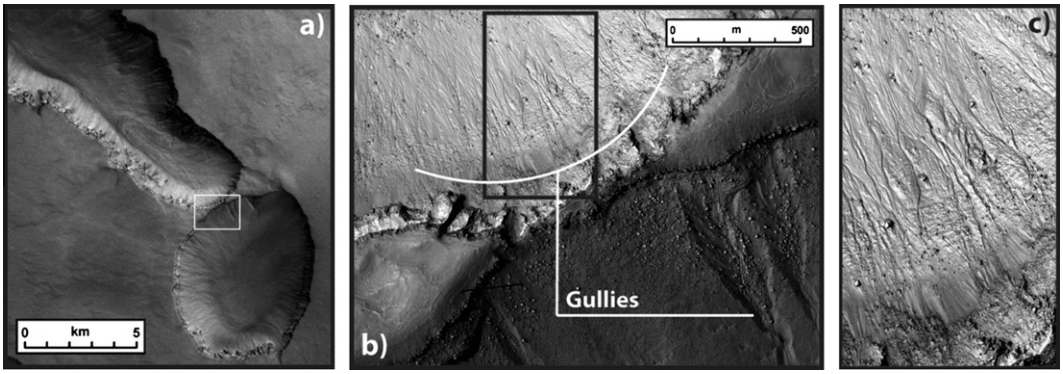

Fig. 10. Isolated ridge gullies. (a) Gullies eroded into slopes on either side of an isolated ridge along the southern end of the northeastern valley; boxes represent the location of the adjacent images. (b) The occurrence of gullies on an isolated slope here and elsewhere within the study area, argues against a groundwater source for the water that carved the gullies. (c) Enlarged view of gullies in (b), demonstrating that gullies are located along the narrowest portions of the ridge, arguing against their formation via a confined aquifer. Morgan et al. (2010) suggested that the gullies were formed by the melting of snow deposits. The image in (b) also shows the aspect dependence of gully morphology present throughout the valley systems. (a) HRSC: h1932_0000, (b) HiRISE: PSP_003880_1325.

disconnected valleys (Fig. 10), argues against the occurrence of perched aquifers providing the gully water source. Morgan et al. (2010) underlined this observation as an argument in support of an external source of water, and suggested that the melt of atmospherically deposited snow was the most likely candidate for the formation of these gullies.

Smaller gully forms that are only resolvable at HiRISE resolutions are also present along slopes within the lower portions of the valleys. There are two distinct morphological types. The first type is located along the side of boulder-covered mounds on valley floors (Fig. 11). These exhibit the three morphological components (alcove, channel and depositional fan) used to define gullies on Mars by Malin and Edgett (2000a), although they are much smaller than the main gullies within the crater (channel lengths are ~200 m, Fig. 11). The alcoves are 20 m wide and are positioned adjacent to each other in single rows cut into the flanks of the mounds. Narrow <1 m wide channels emerge from the alcoves and maintain straight courses except for gentle meanders around

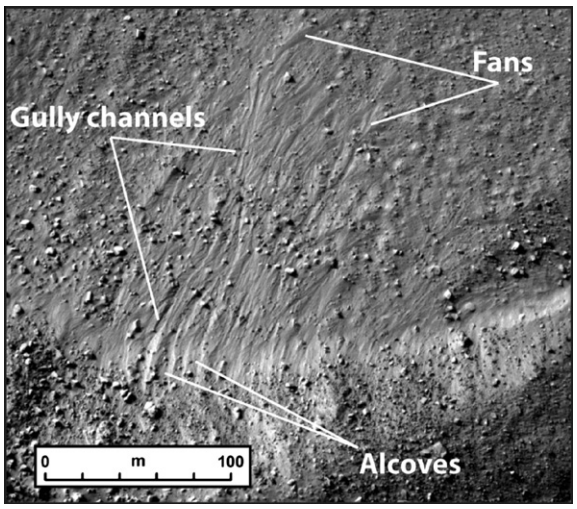

Fig. 11. Small gullies along a debris-covered mound on the floor of the southern valley. The gullies display the three morphologic components of other martian gullies: alcove, channels and fan (Malin and Edgett, 2000a). The small size of these features suggests they are geologically very young, though they might have been active at the same time as the larger gully systems along the upper slopes of the valley walls. HiRISE image: PSP_006926_1320.

boulders (Fig. 11). The slope between the boulders appears smooth and frequently displays fine scale eolian ripples (wavelength of 1 m), suggesting that the gullies are incised into a dust rich layer.

The second type of small gully is located along the side of a dune-covered mound within the southern valley complex (Fig. 12). The dunes are linear with a wavelength of ~3 m. Smaller ripples with a wavelength of ~1 m are present orthogonal to the dune crests, suggesting that the dominant winds that formed the dunes were bidirectional, perpendicular to each other, or that the larger dune forms are relict. The gullies are only comprised of channels, and do not exhibit well-developed alcoves or depositional fans. The channels are ~200 m long, 3 m wide, are bounded by levees, and display largely linear courses except for small-tight meanders (Fig. 12). The level of incision of adjacent channels differs, suggesting that some of the channels were abandoned in favor of other courses. The gullies are orientated in the same direction as the dunes and are of a similar width, suggesting that the dune structure strongly influenced gully formation.

The crisp and unweathered nature of these two groups of gullies, and their small scale, supports the interpretation that they are very young. It is therefore possible that they formed at the same time as the other larger-scale gullies, or alternatively they may result from more recent activity. If they were formed by snowmelt as has been proposed for the larger gullies by Morgan et al. (2010), then smaller volumes of melt would have been required. One explanation for the origin of these smaller gullies (Figs. 11 and 12) may relate to the localized climate effects associated with elevation. The apices of the larger gully alcoves (i.e. the uppermost section of the channels) are at an altitude of around 500 m, whereas the smaller gullies have been found at −1000 m. Both of these values are within the elevation range for gullies that occur elsewhere on Mars (−5000 to +3000 m, Dickson et al., 2007). Nevertheless the 1500 m elevation range between these two gully groups within the study area may be important; the atmospheric lapse rate on Mars is low, and so there is no appreciable surface temperature gradient between these two altitudes. However, the atmospheric-pressure decrease with elevation is significant with regard to water stability. Lobitz et al. (2001) derived an expression for the relationship between elevation and surface pressure on Mars, constrained by the Viking 2 Lander pressure measurements:

$$P(z, L_s) = P_{VL2}(L_s) exp(-(z - z_{VL2})/H) \quad (2)$$

where H is the scale height for Mars, 10.8 km, $P_{VL2}(L_s)$ is the surface pressure at the Viking 2 Lander site at solar longitude L_s (fit to a polynomial curve), and z_{VL2} is the MOLA-derived altitude at the Viking 2 Lander site (−4 km). We used this in conjunction with the one-dimensional version of the atmospheric Laboratoire de Météorologie Dynamique (LMD) GCM (Forget et al., 1999) to plot the present annual difference in climate (average pressure, maximum surface temperatures) between the two elevations of gully alcoves in temperature and pressure space (Fig. 13). Assuming both gully types were formed by snowmelt, we chose albedo and thermophysical properties consistent with a thin dust covered snowpack (see Fig. 13 caption for values). Modeling work by Williams et al. (2008, 2009) has demonstrated that a lag of dust would form on the surface of a snowpack under martian conditions due to sublimation. Both elevations experience limited diurnal periods in the spring when conditions are above the triple point, though this period is more significant for the smaller gullies (Figs. 11 and 12). Further modeling is required to determine if these conditions would be sufficient to permit the melting required to form the small gullies (e.g. Williams et al., 2008, 2009).

4.1.2. Comparisons with other martian gullies

Aspect-dependent gully morphology has been documented elsewhere on Mars. Hale Crater, for example, displays the same relationships between well-developed, deeply-incised, pole-facing gullies and smaller, more subdued gully-like forms on equator-facing slopes (Reiss et al., 2009). The origin of the equator-facing features in Hale Crater is unclear (they do not have incised channels, and are superimposed by impact craters) and may be related to the impact event itself, in a manner similar to the proposed formation of Mojave Crater fluvial features (Williams et al., 2004). The gullies

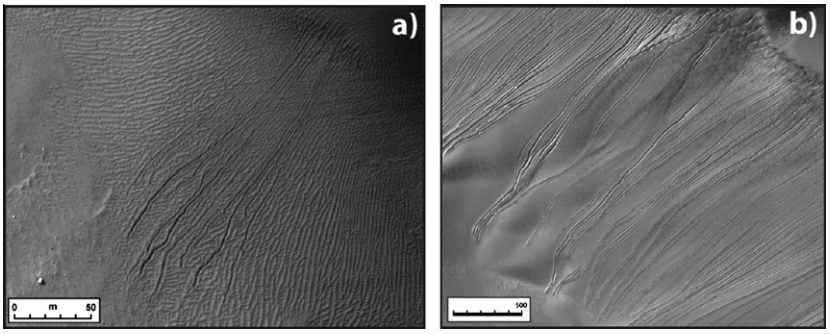

Fig. 12. Small-scale gullies along sand dunes. (a) These gully systems are morphologically different from gullies elsewhere in the study area, although they are similar (despite being an order of magnitude smaller) to gullies observed on Russell Crater dunes (b). Left image: HiRISE: PSP_006926_1320. Right image: HiRISE: PSP_007018_1255.

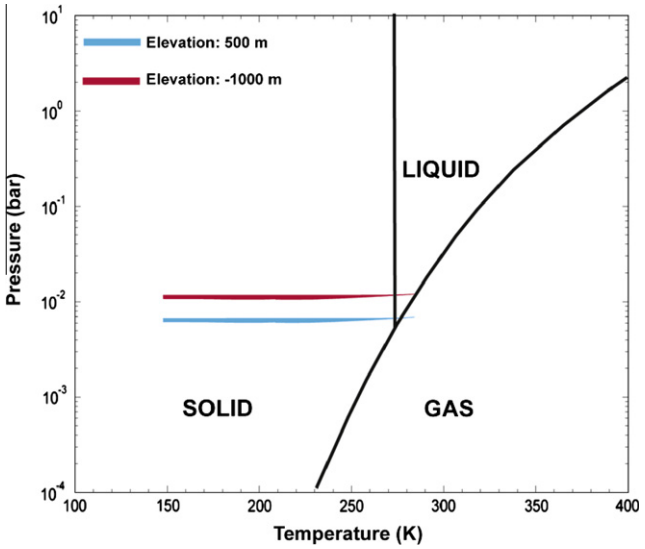

Fig. 13. Phase diagram in temperature and pressure coordinates for water, showing the annual climatic conditions between the top of the valley walls (where the standard gullies originate) and the lower flanks (where the smaller scale gullies originate). Average surface pressures and maximum surface temperatures are plotted for the course of a martian year in each case. The temperatures are the same due to the small martian atmospheric lapse rate, but the elevation difference does have an effect on surface pressures. The plots show that conditions above the triple point are only met for a short period each day during the spring at the elevation of the smaller gullies, and even less for the alcove elevation of the standard gullies. Surface pressures derived from the work of Lobitz et al. (2001). Surface temperatures predicted by the LDM Paris 1D radiative convective model (see Costard et al., 2002). Assuming the gullies are the result of snowmelt, albedo and thermophysical properties of the surface were based on a dirty snowpack covering the slopes. Albedo: 0.15, thermal inertia: 313.

of Asimov Crater, however, are demonstrably younger than the crater and fill material into which they are eroded, and so are not related to the original impact event. Despite the differences in gully morphology as a function of size in Asimov Crater, the large-scale gullies exhibit the basic morphologic characteristic of other mid-latitude gullies as originally documented by Malin and Edgett (2000a), supporting the argument of Morgan et al. (2010) that they were formed during higher obliquity excursions, and in a manner similar to that proposed for gullies elsewhere on Mars (Costard et al., 2002; Christensen, 2003; Dickson et al., 2007; Head et al., 2007, 2008).

The smaller scale gullies of Asimov Crater (Figs. 11 and 12) are only observable at HiRISE resolution, and thus similar examples have not been documented in studies that only rely on MOC imagery. For the gully systems located on lower slopes and near valley floors (Fig. 11), the linked tributary channels imply that water was involved in their formation and that they may simply be scaled-down versions of 'typical' martian gullies documented by Malin and Edgett (2000a). On the other hand, the gullies that occur on along the flanks of sand dunes (Fig. 12) are morphologically similar to larger-scale gully features found on dunes in other regions of Mars. Dune gullies in the study area are compared to those in Russell Crater (55°S, 13°E) in Fig. 12. Both of these gully types have relatively long and thin linear channels and no obvious fan deposits, although the Russell Crater gullies are ~2.5 km long and originate in poorly developed alcoves (Mangold et al., 2003). The Russell dune gullies have been attributed to debris flows initiated by liquid water (Mangold et al., 2003; Reiss and Jaumann, 2004; Miyamoto et al., 2004; Védie et al., 2008), and a similar process may have formed the Asimov "dune" gullies (Fig. 12). Their similar morphology, despite the large difference in scale, may be the result of the two gully sets forming in finer grain-sized, largely unconsolidated deposits as compared to the larger gullies located along the slopes of interior crater walls and valleys. The width of the dune gullies in the study area appears to be controlled by the wavelength of the dunes on which they have formed (Fig. 12), potentially demonstrating the greater influence of dune surface structure at smaller scales.

4.1.3. Age of the gullies

Constraining the age of gullies is difficult because they cover small areas and are limited to steep slopes that are prone to failure. Nevertheless, through the dating of a dune field that has been superposed by gully fans (Reiss et al., 2004), and through the identification and dating of a primary impact crater that has generated secondary impacts on a gully fan (Schon et al., 2009), the most recent episode of gully activity is likely to have occurred <0.5–3 Ma at two separate locations on Mars. Despite the inability to utilize crater counts to provide absolute ages for individual gullies within the study area, crater counts can still be used to compare the relative ages between the different morphological gully types. Morgan et al. (2010) conducted two crater count surveys of equal sized areas, one of polar facing gullies and the other of equator facing. This used all available MOC (22) and HiRISE (8) images for the areas, and revealed that ~70 craters with a diameter >5 m (including six craters with a diameter of >100 m) are superimposed on the fans and channels of gullies on equator-facing slopes relative to only ~15 on the pole-facing gullies. This suggests that the pole-facing gullies have been the most recently active, which is consistent with them being more deeply incised and extensively developed (in terms of tributaries and fine scaled fluvial features) than the simpler equator-facing gullies.

Morgan et al. (2010), in their investigation of gully formation within the study site, used the one-dimensional version of the atmospheric LMD GCM (Forget et al., 1999) to show that the range in gully morphology is correlated with aspect-dependent surface temperature differences that occur during higher obliquities. Their model predicts that the pole-facing gullies could have formed during high obliquity (35°) excursions that occurred periodically over the last 2.5 Ma (Laskar et al., 2004), with the most recent activity potentially occurring ~0.5 Ma. This would place the gullies most recent activity within the age estimates of gully activity by Reiss et al. (2004) and Schon et al. (2009) (see Table 1). However, for equator-facing gullies, Morgan et al. (2010) found that they could only be formed during the periods of highest obliquity that occurred prior to 4 Ma (~45°). Thus, they interpret the cause of the different morphologies to be due to: (1) the longer period of inactivity (potentially 5 Ma for the equator-facing gullies, compared to ~0.5 Ma for the polar facing gullies) and (2) the limited period of activity during each obliquity oscillation prior to 5 Ma for equator-facing gullies (obliquities of 45° were maintained for 20,000 years during each 120 ka obliquity cycle) relative to that of the polar facing gullies (obliquities >35 were maintained for 70,000 years during each ~120 ka obliquity cycle). As of the time of this writing, no recent changes in the appearance of the gullies has been documented from repeated CTX or HiRISE observations. Therefore, there is no evidence to suggest current gully activity. However, Asimov Crater due to its multiple gully systems should be an area of interest in order to test the Morgan et al. (2010) conclusions.

4.2. Lobate debris tongues

4.2.1. Location and morphology

Throughout the valley systems are a series of tongue-shaped, debris-rich lobes that display surface morphological features indicative of viscous flow (Fig. 14). As their origin cannot be directly determined we have chosen to term these features based on their morphological characteristics and refer to them as *lobate debris*

Table 1
Age estimates of gullies and ice-rich flow features on Mars reported in the literature. Note that for crater counts on small surface areas (such as the surface of the smaller ice-rich features: Arfstrom and Hartmann, 2005; LDT), the inferred ages estimates will be broad because of: (1) the uncertainties surrounding the production function of the smallest diameter craters, (2) the effect of secondary craters, and (3) the nature of erosion and deposition (Arfstrom and Hartmann, 2005).

Landform	Location/description	Age estimate	Rationale	Reference
Gullies	Gully fans superimposed on a dune field within Nirgal Vallis at 29°S, 318°E	<0.3–1.4 Ma	Based on crater counts of the dune field	Reiss et al. (2004)
Gullies	Gully fans superimposed on a surface with secondaries at ~35°S, 131°E	<1.25 Ma	Based on crater count age date of a primary crater that had produced secondaries	Schon et al. (2009)
Gullies	Asimov Crater: gullies display strong aspect dependent morphology	Pole-facing gullies >0.5 Ma. Equator-facing gullies >5 Ma	Based on correlation with Laskar et al. (2004) simulations of obliquity variations, suggests pole-facing gullies >0.5 Ma, equator facing gullies >5 Ma	Morgan et al. (2010)
Lobate flow features	*Viscous-flow features* (VFF). Mid-latitudes in both hemispheres	0.1–30 Ma (stratigraphic association with latitude-dependent mantle suggests a similar age: 0.4–1.25 Ma)	Based on average strain rates for viscous flow within a 10 m thick dust-rich icy layer under martian conditions	Milliken et al. (2003)
Lobate flow features	*Glacial like features* (GLF) (presumably of similar origin to VFF documented in Milliken et al. (2003)) in crater at 40°S, 67°E	~<10 Ma	Crater counts	Arfstrom and Hartmann (2005)
Lobate flow features	Debris-covered glaciers along the NW edge of the Olympus Mons scarp	~>5 Ma	Crater counts	Neukum et al. (2004) and Head et al. (2005)
Lobate flow features	Lobate Debris Tongues in Asimov Crater	>8 Ma	Crater counts	This paper
Lobate flow features	Lobate debris aprons/lineated valley fill. Northern dichotomy boundary	100–500 Ma	Crater counts	e.g. Mangold (2003), Kress and Head (2008) and Morgan et al. (2009)

tongues (LDT), by comparison to other similar features on Mars and Earth. These LDT originate at the heads of valleys (Fig. 14), extend for several kilometers, and terminate on valley floors. They exhibit convex-upward topographic profiles and fold-like, compressional-surface ridges (Fig. 14c and inset), suggesting that they have experienced ductile deformation during downslope flow. In some cases, smaller-scale tributary flows have contributed to the formation of large-scale lobate features (Fig. 14b) indicating that integrated flow from several sources has occurred. All of these factors suggest that the lobate debris tongues contained ice that acted to facilitate the downslope creep of debris.

Due to the relatively small size of the lobate debris tongues (typically 3–5 km in length) it is difficult to make accurate measurements of their topography. The along-track spacing of MOLA shots results in a maximum coverage of 5–10 points in a north–south direction (along-track direction). This number can be significantly less for east–west measurements because of widely spaced orbital tracks. Nevertheless, by extracting points from multiple adjacent orbital tracks, we were able to construct a topographic profile for the specific LDT that occupies the eastern head of the southern-most valley (Fig. 15). Extrapolating the topography of the valley floor below the LDT indicates a maximum thickness for the deposit of ~250 m.

The lobate debris-tongue surfaces are covered with boulders up to ~10 m in diameter. These appear similar in albedo and shape to those originating from the lava beds at the top of the slope (Figs. 5 and 7) and suggests that the lobes include debris shed from these layers. Many of the large boulders (>5 m) on the surface of LDT are surrounded by circular depressions (moats) that are up to ~2 m wide (Fig. 16a–c); moat widths appear to be a function of the size of the block (Fig. 16). Erosional scouring associated with eolian activity appears unlikely as a causal mechanism, as one would then expect the moats to be orientated along the dominant wind direction and to exhibit depositional tails on the lee side of the boulders. Because the blocks appear to be comprised of solid rock derived from the lava-flow layers at the wall summit, and are dark relative to the surrounding finer-grained sediments and dust, we suggest an alternative explanation that calls on preferential sublimation of near-surface ice due to the higher thermal inertia and lower albedo of the boulders. In this model, the boulders act as thermal capacitors, absorbing shortwave solar energy and emitting longwave energy, increasing the temperature of the surrounding ground surface and enhancing nearby sublimation. The Pheonix mission has found evidence for depressions within the ice table below decimeter-scale rocks consistent with the ground ice being in diffusive equilibrium with the atmosphere (Sizemore et al., 2010). Alternatively in terrestrial environments, rocks that reach a critical size can cause the development of ice pedestals due to the shadowing effects of the rock preserving the underlying ice. Hence, modeling work is required to ascertain the most likely response of buried ice to basaltic rocks of this scale on Mars. To our knowledge, boulder moats have not been reported in the literature, and if further research supports our interpretation, such occurrences may provide a useful proxy for the occurrence of near-surface ground ice.

Larger-scale topographic features are also apparent along the surface of the LDT deposits. Parallel troughs, ~200 m wide, are present along the central axis of some of the lobate debris tongues (Fig. 16b). The troughs may be a product of deflation processes and might represent the lowering of the surface due to the loss of ice through sublimation. Smaller scale, linear indentations tens of meters in width that are perpendicular to the inferred flow direction are located along the upper, steeper portions of the LDT (Fig. 14a) The indentations may have formed as the result of strain induced by brittle deformation within the most elevated portions of the lobes.

Linear troughs are found elsewhere in Asimov Crater. To the north of the valley shown in Fig. 14a (see Fig. 16a for context), large troughs are present and display a series of 150 m wide, nested

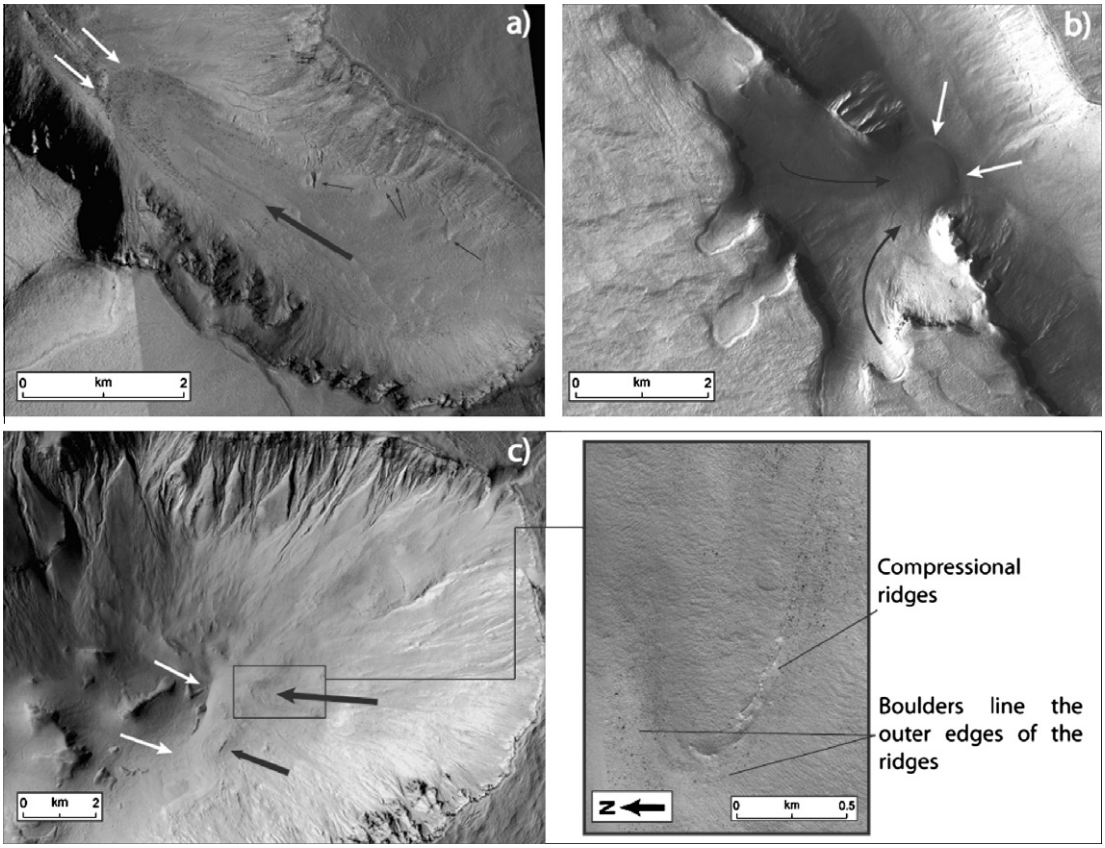

Fig. 14. Examples of lobate debris tongues (LDT) within the study area. White arrows indicate the termini of the lobes, the large black arrows indicate the inferred direction of flow. (a) Four kilometer long LDT within the southern end of the northeastern valley system. Gullies are present along all of the slopes that surround the LDT, the distal ends of the gully channels and their fans curve down along the surface of the lobe. The small black arrows highlight small indentations along the edge of the LDT, which may have formed as the result of strain induced by brittle deformation. HiRISE image: PSP_003880_1325, (b) 3 km long LDT that is fed by smaller tributaries within the western portion of the valley. CTX image: P07_003880_1325, (c) Broad LDT along the eastern end of the southern valley. Compressional ridges can be seen on the surface of the LDT (d). CTX image: P07_003880_1327 (c), HiRISE image: PSP_004091_1325 (d).

concentric terraces (Fig. 16d). Boulders, fringed by moats are present in these troughs. If the troughs and moats are produced in association with sublimation of near-surface ice, as we suspect, then their presence suggests widespread ice-rich material throughout the valleys.

Gullies are found along all slopes from which the lobate debris tongues originate and in some cases the gully fan deposits are emplaced on top of the upper portions of the LDT (Fig. 14a and c and Fig. 15). At the site of the LDT in Fig. 14a, the termini of the gully channels and their fans curve downslope following the direction of advance of the lobe. Despite this general trend, there is one area in the southern valley (Fig. 3) where a LDT appears to be superimposed on top of a gully (Figs. 17 and 18). Along the lower portions of the southern valley, a somewhat degraded gully channel ~40 m wide emanates from below the lobe front of the LDT (Fig. 18). There is a sharp transition between the LDT termini and the upper portions of the gully channel, which suggests that the two features are distinct and that the LDT is not the source of the channel. Understanding the processes by which ice was emplaced to form the LDT, the volume and fate of the ice involved, and the nature of the relationship between the LDT and the gullies is thus essential in the reconstruction of the climate history of the region.

4.2.2. Comparisons with other martian lobate flow features

Lobate/viscous-flow features of various scales that are interpreted to be comprised of ice-rich materials have been identified elsewhere on the martian surface (Squyres, 1978). As described previously these features have been named based on their broad morphological characteristics. We will continue to use the terms put forward in the martian literature, and asses where the LDT fit into this range of ice-rich features.

Two types of the largest lobate/viscous-flow features are: *lobate debris aprons* (LDA) and *lineated valley fill* (LVF). These are found at ~30–50° latitude in both hemispheres, and have been interpreted to be either ice-assisted creep of talus (e.g., Squyres, 1978), or deposits from debris-covered glaciers (e.g. Head et al., 2006a,b). Lobate debris aprons form extensive deposits along scarps and around isolated mesas (Squyres, 1979; Pierce and Crown, 2003) and appear to be genetically related to lineated valley fill, which forms large-scale integrated patterns and extends for hundreds of kilometers through fretted valleys (Head et al., 2006a,b, 2010; Morgan et al., 2009). However, unlike LDA and LVF, the LDT of Asimov Crater are an order of magnitude smaller and display different surface textures, consisting of large boulders and linear troughs. Although LVF/LDA deposits show evidence for flow, they also have pits and buttes that are interpreted to be related to large-scale sublimation processes (Mangold, 2003), features that are not observed on the LDT. Additional LDT traits not typically shared by LVF/LDA deposits (e.g. Head et al., 2010) include (1) the occurrence of large numbers of gullies in the vicinity of the tongue, and (2) a paucity of superposed modified impact craters. LDA/LVF have numerous superposed craters and ages in excess of 100 myr (e.g., Mangold, 2003; Morgan et al., 2009; Kress and Head, 2009). Many of these craters display unique degradational morphologies such as 'oyster shell' (Mangold, 2003) and 'ring-mold' craters (Kress and Head, 2008), both of which are interpreted to be indicative of buried ice.

Milliken et al. (2003) reported on the presence of young *viscous-flow features* (VFF) that are similar in scale to the LDT, and that

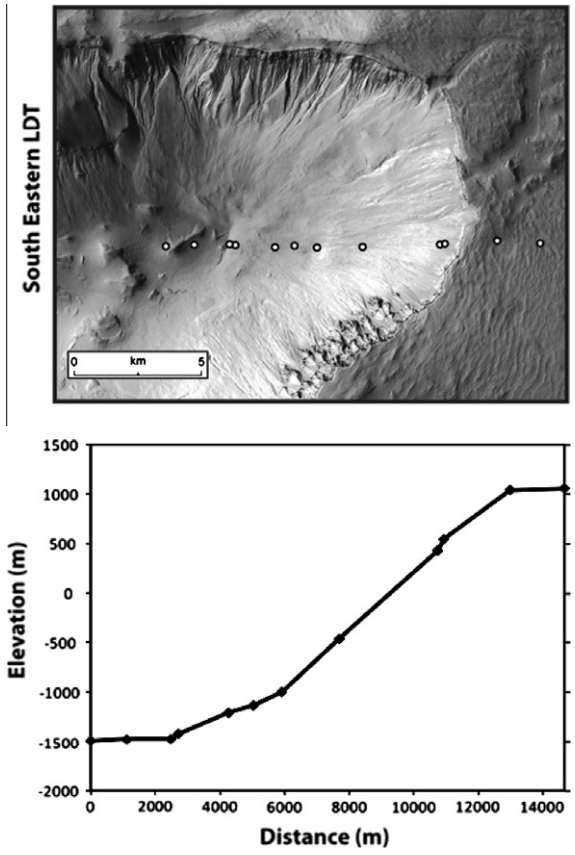

Fig. 15. Topographic transect of LDT along the eastern edge of the southern valley (a), and accompanying MOLA profile (b). The topographical profile was derived from extracting adjacent MOLA points from different orbital tracks. HiRISE image: P06_003313_1327.

show a close association with gullies (Milliken et al., 2003; Head et al., 2003, 2008; Arfstrom and Hartmann, 2005; Reiss et al., 2009). Milliken et al. (2003) identified ~10-m thick viscous-flow features throughout the 30–60° latitude bands which they interpreted to be related to be remnants of ice-rich dust deposits associated with the climate-related, latitude-dependent mantle (Mustard et al., 2001; Head et al., 2003). In a manner very similar to the relationship between LDT and gullies in Asimov Crater, Milliken et al. (2003) documented gullies that cut through the VFF, suggesting a younger age for the gullies and that the gullies may have formed by the melting of ice in the latitudinal dependent mantle. These VFF are significantly thinner than the LDT (i.e. ~10 m for the former compared to ~250 m for the latter) and contain fewer boulders, most likely due to the VFF being composed of more dust-rich material compared to the rocky material that constitutes at least the surface of the LDT.

Additionally, in some craters, gully systems are found to terminate within, and be superimposed on, arcuate depressions at the head of other lobate/viscous-flow features that extend away from the inner walls of craters (Milliken et al., 2003; Head et al., 2008). The arcuate depressions likely reflect modification of debris-covered glaciers, and are inferred to represent enhanced sublimation in former ice-accumulation zones, producing deep hollows that lie well below the level of remaining debris-covered ice in the downslope direction (Head et al., 2008; Marchant and Head, 2007). Overall, these viscous-flow features with irregular hollows differ in shape, setting, and morphology to the LDT described here. Thus, they are considered to represent a different landform type.

Although there is abundant geomorphic evidence that LDA/LVF represent debris-covered glaciers (e.g. Head et al., 2006a,b, 2010), a conclusion recently confirmed with SHARAD radar data (Holt et al., 2008; Plaut et al., 2009), determining the amount of ice present in debris-rich viscous-flow features from morphology alone is a difficult challenge on both Earth and Mars (Whalley and Azizi, 2003; Mangold, 2003; Li et al., 2005; Pierce and Crown, 2003; Shean et al., 2007b). Relevant questions include: (1) How much ice is required to cause mobilization and flow? (2) In what configuration does ice occur (e.g., as pore-ice infilling voids, or as massive ice as in the case of debris-covered glaciers?) (3) Do the currently observed features still contain ice that existed at the time of their formation, or have they lost some or all of this ice? (4) What nomenclature best applies to the description of these features (e.g., Whalley and Azizi, 2003)? Recent work in the Antarctic Dry Valleys has helped to clarify some of these questions. Documentation of the characteristics of debris-covered glaciers in Beacon Valley, Antarctica (Shean et al., 2007b; Levy et al., 2007; Marchant et al., 2010; Shean and Marchant, 2010), and criteria for distinguishing these from other lobate/viscous-flow features formed there (Marchant and Head, 2007; Swanger et al., 2010), leads to a further understanding of the range of candidates and an appropriate nomenclature. We prefer to use the term "debris-covered glacier" where geological evidence supports the presence of subsurface ice that is significantly in excess of pore space and that is demonstrably related to glacier formation (see Head et al., 2010). Evidence supporting debris-covered glaciers includes laterally continuous and converging flow textures and structures (Head et al., 2006a,b), large sublimation pits and unusual superposed craters (Kress and Head, 2008), sublimation polygon structures and their geometry (Marchant et al., 2002; Levy et al., 2006), topographic profiles (Li et al., 2005), detection of abundant subsurface ice by radar (Holt et al., 2008; Plaut et al., 2009) or seismic surveys (Shean et al., 2007b), and experimental and rheological considerations (Mangold and Allemand, 2001; Mangold, 2003; Swanger et al., 2010). We prefer to use the term "rock glacier" where rocky viscous-flow features do not meet these criteria. By these criteria, "rock glaciers" could be either talus deposits mobilized by interstitial ice, or "debris-covered glaciers" that have lost their ice due to sublimation and/or melting, and deflated to their currently observed configuration.

Understanding the source of ice associated with the formation of the LDT and establishing potential sources of water that produced the gully systems is fundamental to deriving the climate conditions under which they both formed. Groundwater injection into debris fans has been proposed as a potential bottom-up source of ice for lobate flow features on Mars (e.g. Mangold and Allemand, 2001). For example, if water was derived from the subsurface in sufficient volumes, it could saturate the pore spaces of debris and/or produce ice lenses; this might enable ice-assisted creep in a manner similar to terrestrial rock glaciers (Whalley and Azizi, 2003). For such a mechanism to operate in Asimov Crater, perched aquifers in communication with the walls of the valleys would be required. The occurrence of gullies and LDT along isolated ridges (Fig. 10), however, is inconsistent with groundwater sources and instead argues for an external, atmospherically linked, top-down, source of ice (see Section 4.1.1).

In summary we propose that (1) Due to the uncertainties associated with distinguishing the origin and volume of ice involved in the formation of flow features on Earth, we are cautious to provide a definitive origin for the LDT. Nevertheless, the occurrence of elongated depressions >1 km wide and rock moats are both suggestive of the loss of excess subsurface ice that was possibly glacial in origin. (2) Assuming that glacial ice was involved in the formation of the LDT, the surface morphology and scale differences between LDT and LVF/LDA may be due to differences in the composition and relative thickness of the surficial till relative to the underlying ice. (3) The occurrence of LDT along isolated ridges

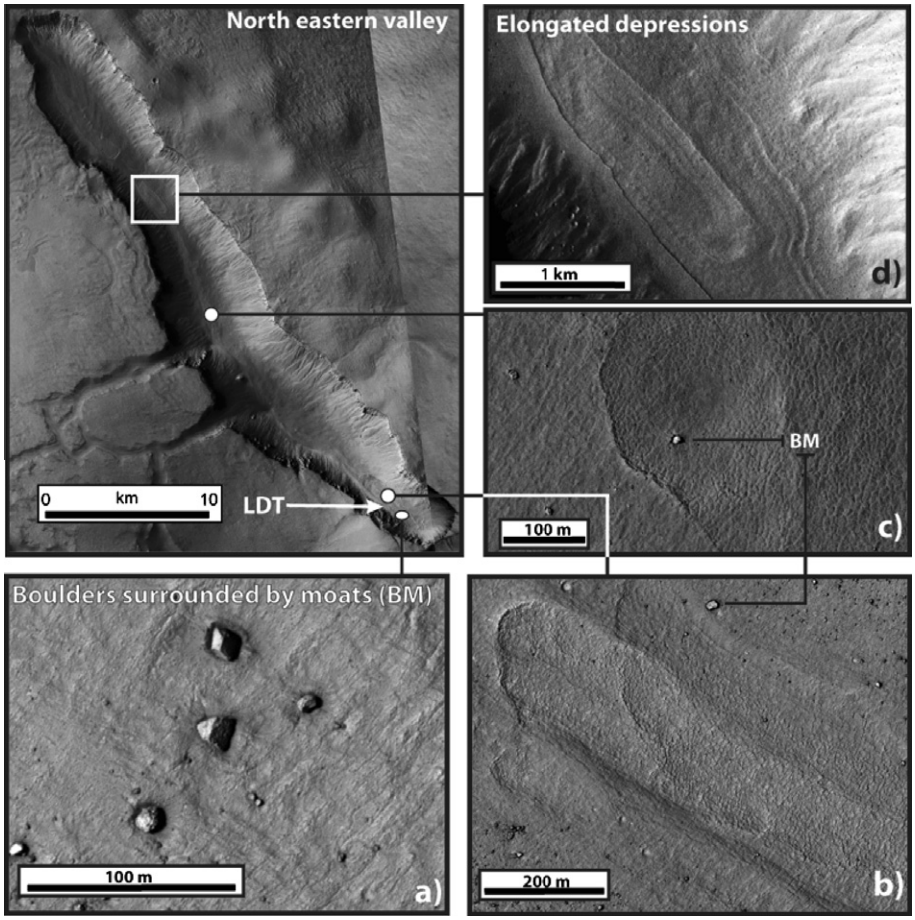

Fig. 16. Features interpreted to be ice-related, along the surface of LDT and the floors of the adjacent valleys. (a) Large boulders (>5 m) on the surface of the LDT have moats surrounding them; these may be formed due to the loss of near-surface ice, via sublimation as a result of the thermal properties of the rocks. (b) Elongated troughs, 200 m wide that are parallel to the long axis of the LDT. The troughs may have been formed by the lowering of the LDT surface as a result of the loss of subsurface ice through sublimation. (c) Similar trough to (b) along the floor of the valley to the north of the LDT. (d) Further to the north, concentric troughs form 50 m wide stepped terraces. Boulders with moats are also present along the floor of the valley. The occurrence of these features on LDT and the floor of the valleys suggest that both features contain near-surface ice and presumably formed in the same manner via the accumulation of ice and debris. Context image and (d) CTX image: P07_003880_1327. Other images, subsets of HiRISE image: PSP_003880_1325.

rules out a groundwater source and suggests that the LDT were formed by an atmospherically derived source of ice. The outstanding questions are what is the volume of the ice involved and when did it accumulate in Mars history? For example, could the LDT be deflated debris-covered glaciers formed by post-emplacement loss of ice by vapor diffusion through the overlying sublimation till?

4.2.3. Age of lobate debris tongues

The superposition of gullies along the upper portions of the LDT (with the exception of possibly one gully, see Figs. 17 and 18) indicates that the gullies are predominantly younger than the LDT. Thus a period of gully formation is interpreted to have followed the emplacement of the LDT. The larger scale and lower slope of the surface of the LDT relative to the gully systems makes it possible to make crater count surveys to provide minimum age estimates. Crater counts and crater size–frequency distributions were compiled for a lobate debris tongue in order to derive an age for the surface of the feature. One hundred craters were identified on the surface of the LDT; the largest crater had a diameter of ~30 m.

The position of the largest diameter crater bin falls on the 8 Ma isochron suggesting that this represents a minimum age for the surface (Fig. 19). The significant rollover in smaller craters (<10 m D) is possibly due to a modification of the surface since the LDT was emplaced (this might be related to ice loss as is hypothesized for the formation of the linear troughs on the surface of the LDT, Fig. 16). Thus the age above relates to the modification of the surface, so the actual age of the formation of the LDT is likely to be significantly older than this.

5. Discussion: interpretation of the local climate history

The age of the LDT inferred from crater counting (surface age >8 Ma, Fig. 19) suggests that they are older than the most recent period of ice-rich mantle formation associated with the last martian 'ice age' (0.4–2.1 Ma, obliquity ~35°; Head et al., 2003) and thus the LDT could not have formed during this time as has been suggested for other small lobate flow features (Milliken et al., 2003; Arfstrom and Hartmann, 2005, see Table 1 and Fig. 20). The age of the LDT overlaps with that of the youngest glaciers deposits, superimposed on the debris-covered piedmont glaciers at the base of Olympus Mons (Neukum et al., 2004; Head et al., 2005; Milkovic et al., 2006). These younger glacial lobes are very similar to debris-covered glaciers in Antarctica (Head et al., 2005, their Fig. 3; Marchant and Head, 2007). The crater counts also place the formation of the LDT prior to the increase in average obliquity to ~35° (Fig. 20) that occurred ~5 Ma (Laskar et al., 2004). At obliquities higher than 45° the redistribution of ice is expected to have become more pronounced and the resulting migration in ice stability (Mellon and Jakosky, 1995) may have facilitated the deposition

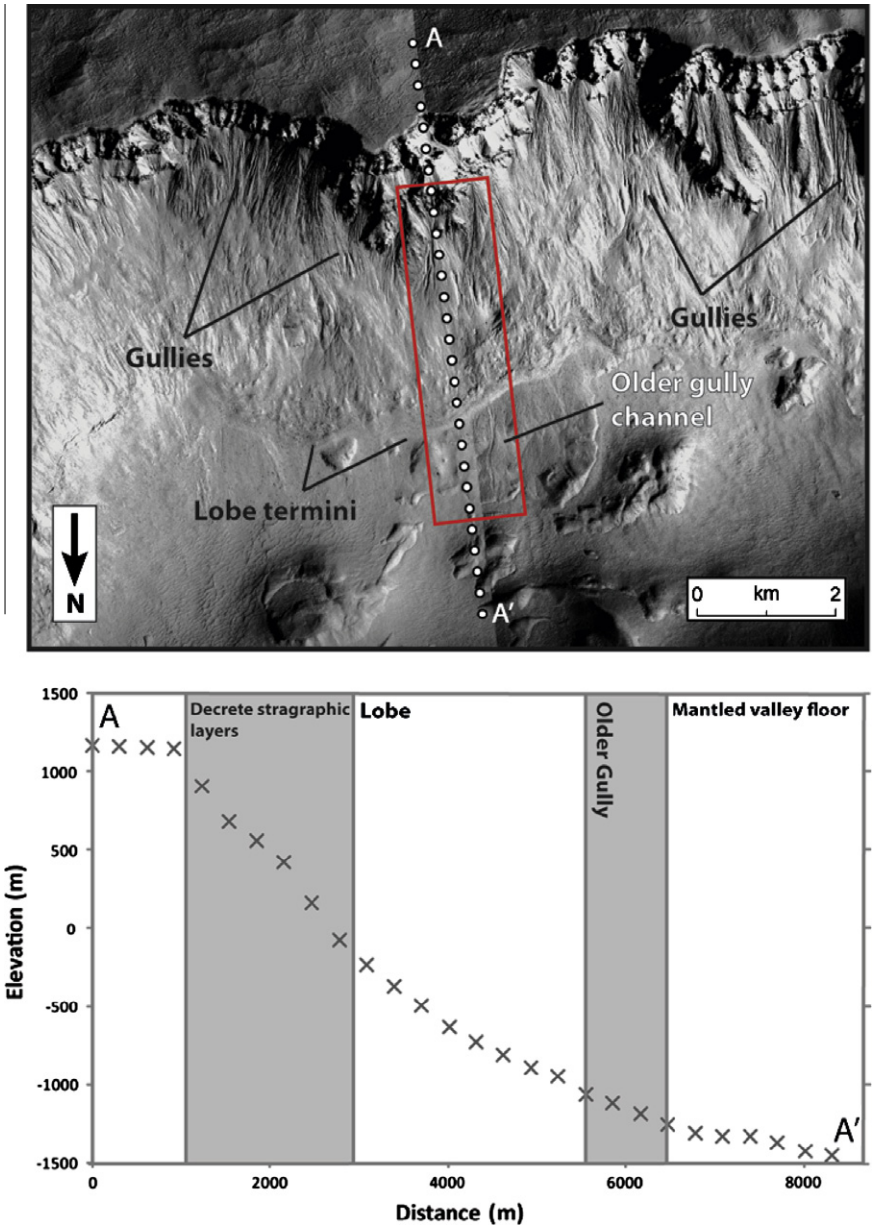

Fig. 17. Image and accompanying MOLA profile of a portion of the southern wall of the southern valley that shows a degraded LDT superimposed on a relict gully channel. Gullies are also superposed on the surface of the LDT, opening the possibility that the formation of the LDT postdated a previous period of gully formation or occurred during an extended gully formation period. Composite of CTX images. The box represents the location of the image in Fig. 18.

of thick ice deposits at the mid-latitudes (Head et al., 2006a,b; Madeleine et al., 2007). This is relevant to the LDT providing Mars experienced similarly high obliquity values during their formation >8 Ma. If this was the case the direct deposition of this ice onto the walls of the valleys or the calving of ice from deposits above the cliff at the summit of the slopes may have enabled the formation of small glaciers in the valleys. Debris supplied to the surface of the lobes from mass wasting along the cliffs above could have buried ice-rich material and protected it from sublimation in a manor similar to that described for the preservation of the Olympus Mons debris-covered glaciers (Head et al., 2005). The subsequent downslope movement of this material could have resulted in the LDT preserved today.

The occurrence of a similar texture and features interpreted to be related to the occurrence of near-surface ice (e.g. boulders with moats and elongated depressions, see Fig. 16) along the floor of valleys <5 km wide to those present on the surface of the LDT suggests that ice-rich deposits may also be preserved within these valleys. Such deposits could have been formed the same way as the LDT, except that the lack of a steep topographic gradient prevented the formation of obvious flow features (e.g. compressional ridges). The absence of these features within the wider valleys (such as the southern valley) is logical as the floors of narrower valleys would be more sheltered from insolation and would receive higher amounts of debris due to the closer proximity of the valley walls, and therefore would provide a higher preservation potential for buried ice. The preservation of ice within the narrower valleys may in part explain their shallower cross sectional profiles relative to the southern valley (Fig. 4).

Once the source of ice was cut off to the valley slopes, the LDT would be dominated by sublimation, which, in turn is dictated by the thickness and porosity of the debris layer above the ice (Kowalewski et al., 2006). We attribute the loss of ice from the LDT as the reason for the downturn of small craters in the crater size–frequency

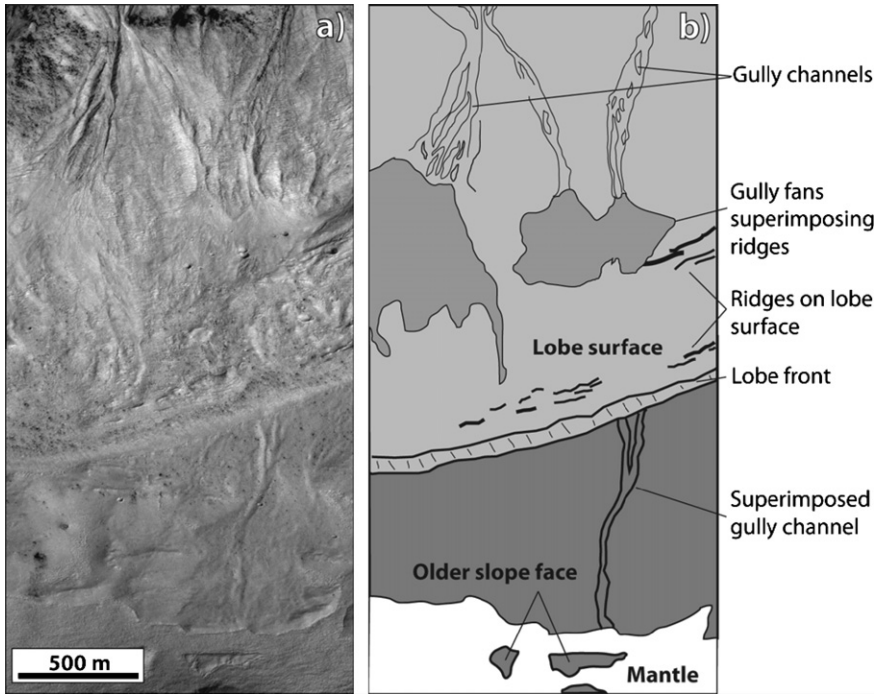

Fig. 18. Image (a) and accompanying sketch map (b) showing a potential relict gully channel that is stratigraphically beneath a degraded LDT. This suggests that at least some gully activity was occurring prior to the formation of the LDT. Elongated ridges are also present along the surface of the lobe. MOC image: M1101304.

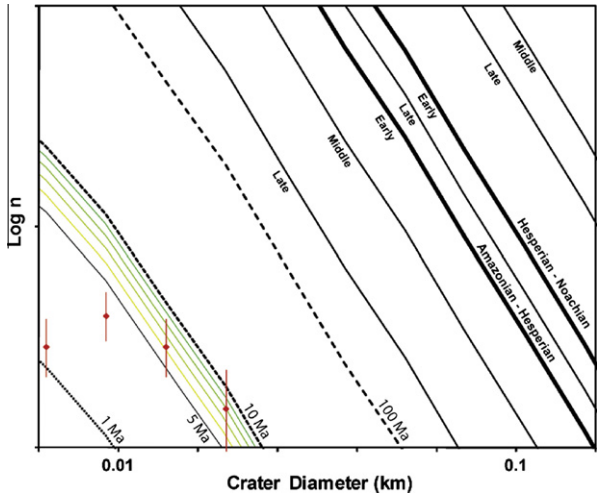

Fig. 19. Crater size–frequency distribution diagram for craters counted on the surface of a LDT (Fig. 14a). The counts suggest a surface age for the LDT of >8 Ma. The reason for the poor fit of the crater size distribution with the isochrons may result from the surface modification of the LDT since its original emplacement. Isochrons plotted according to Hartmann (2005).

distribution plots (Fig. 19). If an ice core was present within the LDT, the effects of ablation of that ice and the associated deflation of the lobe would leave debris stranded on the valley floor and vulnerable to aeolian deflation. Further ablation could cause subsidence of the surface and generate the elongated depressions that are observed on the surface of the LDT and the floors of the thinner valleys. These are similar to 'spoon depressions' observed in terrestrial debris-covered glaciers that have undergone enhanced ablation (Whalley and Azizi, 2003). This may indicate that ice sublimation is ongoing, and that ice has been preserved within some of the LDT and valley floors for ~8 Ma (Fig. 19). This level of ice preservation beneath a debris layer is consistent with geomorphic (Head et al., 2006a,b) and ground probing radar (Plaut et al., 2009) data that support the 100–500 Ma preservation of large bodies of glacial ice below a relatively thin sublimation lag within LDA/LVF deposits (e.g. Mangold, 2003; Morgan et al., 2009, see Fig. 20).

The modeling work of Morgan et al. (2010) suggests that the major gully systems in Asimov Crater (i.e. not including the small-scale features found on the valley floor; Figs. 11 and 12) were active during periods of high obliquity throughout recent martian history. The level of activity is interpreted to be dependent on the aspect of the gullies, with the most recent activity limited to the pole-facing slopes and occurring as recently as ~0.5 Ma. These age estimates are consistent with other estimates of gully activity (Reiss et al., 2004; Schon et al., 2009, see Table 1) and demonstrate the significant difference in age between the gullies and the LDT. Fieldwork conducted in the ADV has shown that gully activity can occur due to the melt of small-scale snow banks (Head et al., 2007; Morgan et al., 2008). Therefore, gully activity requires substantially less ice than is required for the LDT formation, and unless there were prolonged periods of low obliquity, gullies are likely to have been forming since the initiation of the LDT. The aspect dependence of gully morphology has also had an apparent affect on the gradient of the slopes on the valleys (Fig. 2c). Pole facing slopes are generally gentler and are correlated with the largest and most complex gullies, which appear to have assisted the downslope movement of material. Due to this factor, the modification of the LDT in Fig. 14a by gully activity has been more substantial along the pole-facing slopes.

The occurrence of a potentially relict gully channel below a LDT is intriguing (Figs. 17 and 18). One possibility is that the channel relates to a period of gully activity that occurred prior to the initiation of the LDT. Statistical analysis of the evolution of Mars' obliquity has shown 37.62° to be the average value for the last 5 Ga (Laskar et al., 2004). This value is consistent with gully formation models (e.g. Costard et al., 2002) and demonstrates that gully activity may have occurred >8 Ma (age of LDT formation). If this is correct, the formation of LDT might represent a limited period in which the deposition of large volumes of ice in the mid-latitudes occurred. Alternatively the relict channel may be related to the LDT

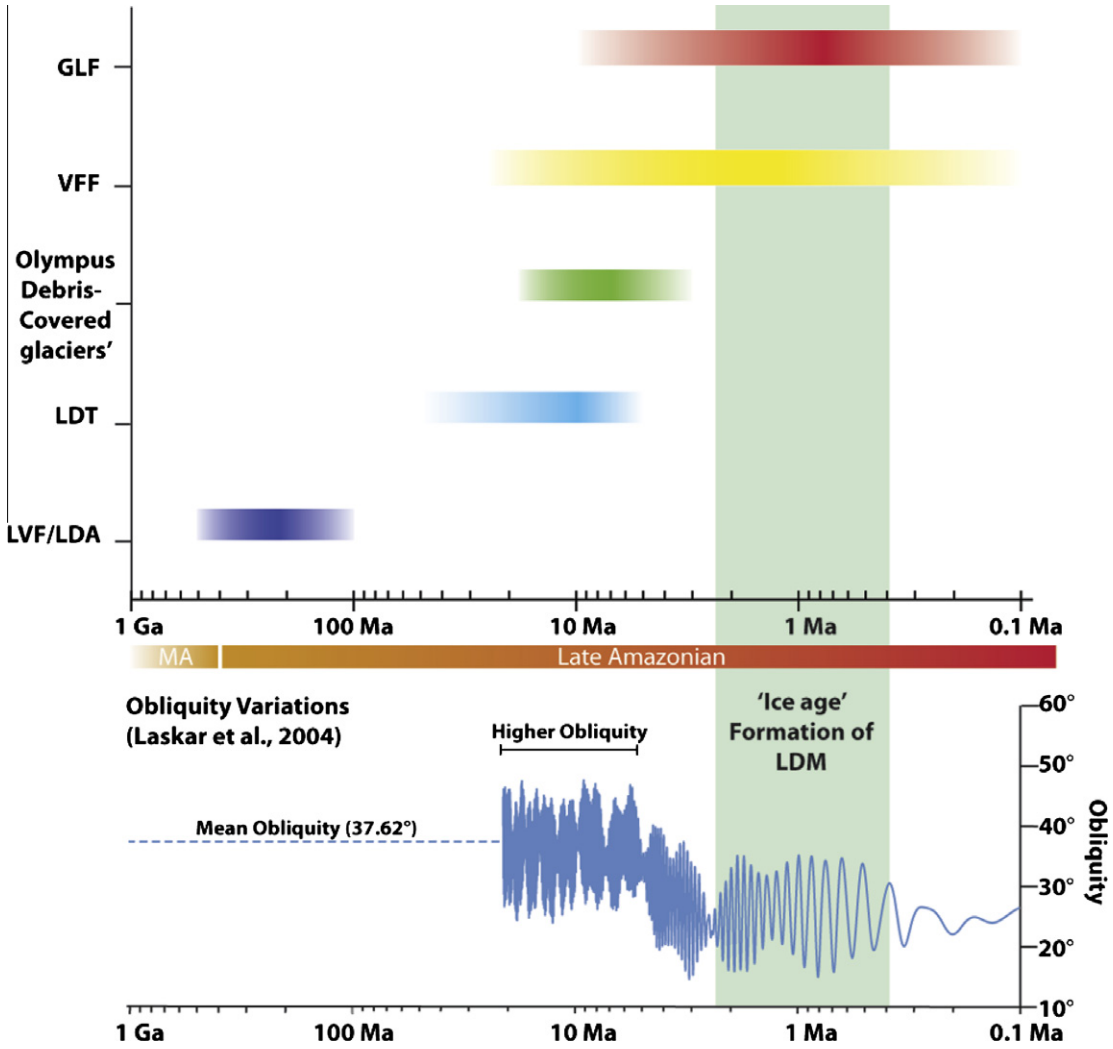

Fig. 20. Comparisons between the age of the LDT and the age of other lobate viscous-flow features on Mars (see Table 1 for more details). Crater counts of the surface of the LDT (Fig. 19) reveal that it has an age >8 Ma. This is prior to the most recent period of high obliquity that has been interpreted to have deposited the latitude-dependant mantle (LDM) during an 'ice age' (Head et al., 2003) and formed both the viscous-flow feature (VFF) (Milliken et al., 2003) and glacier like features (GLF) (Arfstrom and Hartmann, 2005). It is important to note that uncertainties regarding the upper age limits of VFF and GLF mean that we cannot rule out their emplacement as being contemporaneous with the LDT. The figure also points out that the LDT formed prior to the transition from higher obliquity (average ~35°) to lower obliquity (average value ~25°), suggesting possibly that a period of higher obliquity peaks was instrumental in LDT formation. The LDT age overlaps with that estimated for the Olympus Mons debris-covered glaciers (Head et al., 2005), opening up the possibility that they both formed during the same climatic period. The plot also demonstrates the likely younger age of the LDT relative to LVF and LDA deposits, suggesting that large-scale glacial deposition has not occurred over the most recent period of the Late Amazonian. Obliquity plot from Laskar et al. (2004). Obliquity becomes non-deterministic prior to ~20 Ma; nevertheless statistical assessment of the possible values demonstrates that the average value of obliquity over the last 5 Ga was likely to be ~37.6°.

lobe, and therefore might be representative of the melting of ice within the LDT. Milliken et al. (2003) suggested that VFF may have provided a source of water to gullies elsewhere on Mars. No other more ancient channels were found in proximetry to LDT termini. Therefore, if melting had occurred it does not appear to have been widespread. Nevertheless, the occurrence of small fluvial channels in association with lobate features or gully forms that appear stratigraphically older than typical Malin and Edgett (2000a) gullies should be a target for future surveys using high resolution data sets.

6. Conclusions

Our research underlines the potential for ice-related landforms on Mars to be used to derive information about climatic changes that occurred during the Amazonian period of the history of Mars. The study site has experienced a long and diverse geological history, involving the formation of a Noachian crater, its subsequent infill by sedimentary material, and its capping by thick lava flows in the Noachian and Hesperian. Although the process of formation of the valleys is still a matter of debate, the valleys themselves have produced a unique environment in which to study the geomorphic signals of climate change. The occurrence of steep slopes (>20°), relatively narrow (hence sheltered) valleys, and a source of debris has provided favorable conditions for the preservation of ice and the formation of gullies within preferential insolation environments. Analysis of Asimov Crater valleys has led to the identification of a distinctive class of features; lobate debris tongues (LDT). These are small-scale, ice and debris-rich flow features, and their emplacement largely predates the formation of gullies.

The observed morphologic changes are best explained as a shift in martian climate from one compatible with excess snowfall, accumulation and flow of ice-rich deposits, to one incompatible with excess snowfall and lobate tongue formation, but consistent with minor snowmelt and gully formation (see also Head et al., 2008). Available dating suggests that the climate transition

occurred >8 Ma, prior to the formation of other small-scale ice-rich flow features identified elsewhere on Mars that have been interpreted to have formed during the most recent phases of high obliquity. This suggests that multiple climatic shifts may have occurred over the last tens of millions of years of martian history.

Acknowledgments

We gratefully acknowledge financial support from the NASA Mars Fundamental Research Program (NASA MFRP NNX06AE32G) and the NASA Mars Data Analysis Program (NNG05GQ46G). We thank Vic Baker and Alfred McEwen for reviews which significantly improved the manuscript. We are also grateful to Caleb Fassett and James Dickson for their technical contribution to the preparation of the manuscript and useful insights during scientific discussions.

References

Arfstrom, J., Hartmann, W.K., 2005. Martian flow features, moraine-like ridges, and gullies: Terrestrial analogs and interrelationships. Icarus 174, 321–335.
Baker, V.R., 2001. Water and the martian landscape. Nature 412, 228–236.
Bibring, J.-P. et al., 2006. Global mineralogical and aqueous Mars history derived from OMEGA/Mars Express data. Science 312, 400–404.
Cabrol, N.A., Grin, E.A., 1999. Distribution, classification and ages of martian impact crater lakes. Icarus 142, 160–172.
Carr, M.H., 1996. Water on Mars. Oxford Univ. Press, USA.
Chorley, R.J., Schumm, S.A., Sugden, D.E., 1985. Geomorphology. Routledge, UK.
Christensen, P.R., 2003. Formation of recent martian gullies through melting of extensive water-rich snow deposits. Nature 422, 45–48.
Costard, F., Forget, F., Mangold, N., Peulvast, J.P., 2002. Formation of recent martian debris flows by melting of nearsurface ground ice at high obliquity. Science 295, 110–113.
Degraff, J.M., Long, P.E., Aydin, A., 1989. Use of joint-growth directions and rock textures to infer thermal regimes during solidification of basaltic lava flows. J. Volcanol. Geotherm. Res. 38, 309–324.
Dickson, J.L., Head, J.W., Kreslavsky, M., 2007. Martian gullies in the southern mid-latitudes of Mars: Evidence for climate-controlled formation of young fluvial features. Icarus 188, 315–323.
Diniega, S., Byrne, S., Bridges, N.T., Dundas, C.M., McEwen, A.S., 2010. Present-day martian dune gully activity. Lunar Planet. Sci. 41, 2216.
Dundas, C.M., McEwen, A.S., Diniega, S., Byrne, S., 2010. New and recent gully activity on Mars as seen by HiRISE. Geophys. Res. Lett. 37. doi:10.1029/2009GL041351.
Fassett, C.I., Head, J.W., 2007. Layered mantling deposits in northeast Arabia Terra, Mars: Noachian–Hesperian sedimentation, erosion and terrain inversion. J. Geophys. Res. 112, E08002. doi:10.1029/2006JE002875.
Forget, F., Hourdin, F., Fournier, R., Hourdin, C., Talagrand, O., Collins, M., Lewis, S.R., Read, P.L., Huot, J.-P., 1999. Improved general circulation models of the Martian atmosphere from the surface to above 80 km. J. Geophys. Res. 104 (E10), 24155–24175.
Forget, F., Haberle, R.M., Montmessin, F., Levrard, B., Head, J.W., 2006. Formation of glaciers on Mars by atmospheric precipitation at high obliquity. Science 311, 368–371.
Garvin, J.B., Sakimoto, S.E.H., Frawley, J.J., 2003. Craters on Mars: Global geometric properties from gridded MOLA topography. Sixth International Conference on Mars. Abstract 3277.
Grossenbacher, K.A., McDuffie, S.M., 1995. Conductive cooling of lava: Columnar joint diameter and stria width as functions of cooling rate and thermal gradient. J. Volcanol. Geotherm. Res. 69 (1–2), 95–103.
Hartmann, W.K., 2005. Martian cratering 8: Isochron refinement and the chronology of Mars. Icarus 174, 294–320.
Head, J.W., Marchant, D.R., 2003. Cold-based mountain glaciers on Mars: Western Arsia Mons. Geology 31, 641–644.
Head, J.W., Mustard, J.F., Kreslavsky, M.A., Milliken, R.E., Marchant, D.R., 2003. Recent ice ages on Mars. Nature 426, 797–802.
Head, J.W., and 12 colleagues, HRSC Co-Investigator Team, 2005. Tropical to mid-latitude snow and ice accumulation, flow and glaciation on Mars, Nature 434, 346–351.
Head, J.W., Marchant, D.R., Agnew, M.C., Fassett, C.I., Kreslavsky, M.A., 2006a. Extensive valley glacier deposits in the northern mid-latitudes of Mars: Evidence for Late Amazonian obliquity-driven climate change. Earth Planet. Sci. Lett. 241, 663–671.
Head, J.W., Nahm, A.L., Marchant, D.R., Neukum, G., 2006b. Modification of the dichotomy boundary on Mars by Amazonian mid-latitude regional glaciation. Geophys. Res. Lett 33, L08S03. doi:10.1029/2005GL024360.
Head, J.W., Wilson, L., Dickson, J.L., Neukum, G., and HRSC Co-Investigator Team, 2006c. The Huygens-Hellas giant dike system on Mars: Implications for Late Noachian–Early Hesperian volcanic resurfacing and climatic evolution. Geology 34, 285–288. doi:10.1130/G22163.1.
Head, J.W., Marchant, D.R., Dickson, J., Levy, J., Morgan, G., 2007. Transient streams and gullies in the Antarctic Dry Valleys: Geological setting, processes and analogs to Mars. In: Cooper, A.K., Raymond, C.R., the ISAES team (Eds.), Antarctica: A Keystone in a Changing World – Online Proceedings of the 10th ISAES. USGS Open-File Report 2007-1047, 151, p. 4.
Head, J.W., Marchant, D.R., Kreslavsky, M.A., 2008. Formation of gullies on Mars: Link to recent climate history and insolation microenvironments implicate surface water flow origin. Proc. Natl. Acad. Sci. 105, 13258–13263. doi:10.1073/pnas.0803760105.
Head, J.W., Marchant, D.R., Dickson, J.L., Kress, A., Baker, D.M., 2010. Northern mid-latitude glaciation in the Late Amazonian period of Mars: Criteria for the recognition of debris-covered glacier and valley glacier landsystem deposits. Earth Planet. Sci. Lett., in press. doi:10.1016/j.epsl.2009.06.041.
Hecht, M.H., 2002. Metastability of liquid water on Mars. Icarus 156, 373–386.
Heldmann, J.L., Mellon, M.T., 2004. Observations of martian gullies and constraints on potential formation mechanisms. Icarus 168, 285–304.
Holt, J.W., and 11 colleagues, 2008. Radar sounding evidence for buried glaciers in the southern mid-latitudes of Mars. Science 322, 1235–1238. doi:10.1126/science.1164246.
Irwin III, R.P., Watters, T.R., Howard, A.D., Zimbelman, J.R., 2004. Sedimentary resurfacing and fretted terrain development along the crustal dichotomy boundary, Aeolis Mensae, Mars. J. Geophys. Res. 109, E09011. doi:10.1029/2004JE002248.
Jamieson, S.S.R., Sugden, D.E., 2008. Landscape evolution of Antarctica. In: Cooper, A.K., Barrett, P., Stagg, H., Storey, B., Stump, E., Wise, W., and 10th ISAES Editorial Team (Eds.), Antarctica, A Keystone in a Changing World. The National Academic Press, USA, pp. 39–54.
Kadish, S.J., Head, J.W., Parsons, R.L., Marchant, D.R., 2008. The Ascraeus Mons fan-shaped deposit: Volcano–ice interactions and the climatic implications of cold-based tropical mountain glaciation. Icarus 197, 84–109. doi:10.1016/j.icarus.2008.03.019.
Kieffer, H.H., Zent, A.P., 1992. Quasi-periodic climate change on Mars. In: Kieffer, H.H., Jakosky, B.M., Snyder, C.W., Mathews, M.S. (Eds.), Mars. Univ. of Arizona Press, Tucson, AZ, pp. 1180–1220.
Kowalewski, D., Marchant, D.R., Levy, J.S., Head, J.W., 2006. Quantifying low rates of summertime sublimation for buried glacier ice in Beacon Valley, Antarctica. Antarct. Sci. 18, 421–428. doi:10.1017/S0954102006000460.
Kreslavsky, M.A., Head, J.W., 2000. Kilometer-scale roughness of Mars: Results from MOLA data analysis. J. Geophys. Res. 105, 26695–26712.
Kress, A.M., Head, J.W., 2008. Ring-mold craters in lineated valley fill and lobate debris aprons on Mars: Evidence for subsurface glacial ice. Geophys. Res. Lett. 35, L23206. doi:10.1029/2008GL035501.
Kress, A.M., Head, J.W., 2009. Ring-mold craters on lineated valley fill, lobate debris aprons, and concentric crater fill on Mars: Implications for near-surface structure, composition, and age. Lunar Planet. Sci. 40. Abstract 1379.
Krevslasky, M.A., Head, J.W., Marchant, D.R., 2008. Periods of active permafrost layer formation during the geological history of Mars: Implications for circum-polar and mid-latitude surface processes. Planet. Space Sci. 56, 289–302. doi:10.1016/j.pss.2006.02.010.
Laskar, J., Correia, A.C.M., Gastineau, M., Joutel, F., Levrard, B., Robutel, P., 2004. Long term evolution and chaotic diffusion of the insolation quantities of Mars. Icarus 170, 343–364.
Lee, P., Cockell, C.S., Marinova, M.M., McKay, C.P., Rice, J.W., 2001. Snow and ice melt flow features on Devon Island, Nunavut, Arctic Canada as possible analogs for recent slope flow features on Mars. Lunar Planet. Sci. 32. Abstract 1809.
Levy, J.S., Marchant, D.R., Head, J.W., 2006. Distribution and origin of patterned ground on Mullins Valley debris-covered glacier, Antarctica: The roles of ice flow and sublimation. Antarct. Sci. 18, 385–397. doi:10.1017/S0954102006000435.
Levy, J.S., Head, J.W., Marchant, D.R., Dickson, J.L., Morgan, G.A., 2007. Gully surface and shallow subsurface structure in the South Fork of Wright Valley, Antarctic dry valleys: Implications for gully activity on Mars. Lunar Planet. Sci. 38. Abstract #1728.
Li, H., Robinson, M.S., Jurdy, D.M., 2005. Origin of martian northern hemisphere mid-latitude lobate debris aprons. Icarus 176, 382–394.
Lobitz, B., Wood, B.L., Averner, M.M., McKay, C.P., 2001. Use of spacecraft data to derive regions on Mars where liquid water would be stable. Proc. Natl. Acad. Sci. 98, 2132–2137.
Long, P.E., Wood, B.J., 1986. Structures, textures, and cooling histories of Columbia River basalt flows. Geol. Soc. Am. Bull. 97, 1144–1155.
Madeleine, J.-B., Forget, F., Head, J.H., Levrard, B., Montmessin, F., 2007. Exploring the northern mid-latitude glaciation with a general circulation model. Seventh International Conference on Mars. Abstract 3096.
Malin, M.C., Edgett, K.S., 2000a. Evidence for recent groundwater seepage and surface runoff on Mars. Science 288, 2330–2335.
Malin, M.C., Edgett, K.S., 2000b. Sedimentary rocks of early Mars. Science 290, 1927–1937.
Mangold, N., 2003. Geomorphic analysis of lobate debris aprons on Mars Orbiter Camera scale: Evidence for ice sublimation initiated by fractures. J. Geophys. Res. 108 (E4), 8021. doi:10.1029/2002JE001885.
Mangold, N., Allemand, P., 2001. Topographic analysis of features related to ice in Mars. Geophys. Res. Lett. 28, 407–410.
Mangold, N., Costard, F., Forget, F., 2003. Debris flows over sand dunes on Mars: Evidence for liquid water. J. Geophys. Res. 108 (E4), 5027. doi:10.1029/2002JE001958, 2003.
Marchant, D.R., Head, J.W., 2007. Antarctic Dry Valleys: Microclimate zonation, variable geomorphic processes, and implications for assessing climate change on Mars. Icarus 192, 187–222.

Marchant, D.R., Lewis, A., Phillips, W.C., Moore, E.J., Souchez, R., Landis, G.P., 2002. Formation of patterned-ground and sublimation till over Miocene glacier ice in Beacon Valley, Antarctica. Geol. Soc. Am. Bull. 114, 718–730.

Marchant, D.R., Mackay, S.L., Head, J.W., Kowalewski, D.E., 2010. Documenting microclimate variation and the distribution of englacial debris in Mullins glacier, Antarctica: Implications for the origin, flow, and modification of LDA and LVF on Mars. Lunar Planet. Sci. 41. Abstract 2601.

McEwen, A.S. et al., 2007. A closer look at water-related geologic activity on Mars. Science 317, 1706–1709.

Mellon, M.T., Jakosky, M.B., 1995. The distribution and behavior of martian ground ice during past and present epochs. J. Geophys. Res. 100, 11781–11799.

Mellon, M., Phillips, R., 2001. Recent gullies on Mars and the source of liquid water. J. Geophys. Res. 106, 23165–23179.

Milkovic, S.M., Head, J.W., Marchant, D.R., 2006. Debris-covered piedmont glaciers along the northwest flank of the Olympus Mons scarp: Evidence for low-latitude ice accumulation during the Late Amazonian of Mars. Icarus 181, 388–407.

Milliken, R.E., Mustard, J.F., Goldsby, D.L., 2003. Viscous flow features on the surface of Mars: Observations from high-resolution Mars Orbiter Camera (MOC) images. J. Geophys. Res. 108, 5057–5068.

Miyamoto, H., Dohm, J.M., Baker, V.R., Beyer, R.A., Bourke, M., 2004. Dynamics of unusual debris flows on martian sand dunes. Geophys. Res. Lett. 31, L13701. doi:10.1029/2004GL020313.

Morgan, G.A., Head, J.W., Marchant, D.R., Dickson, J.L., Levy, J.S., 2008. Gully formation and evolution in the Antarctic Dry Valleys: Implications for Mars. Workshop on Martian Gullies, Houston, TX. Abstract 1301.

Morgan, G.A., Head, J.W., Marchant, D.R., 2009. Lineated valley fill (LVF) and lobate debris aprons (LDA) in the Deuteronilus Mensae northern dichotomy boundary region, Mars: Constraints on the extent, age and episodicity of Amazonian glacial events. Icarus. doi:10.1016/j.icarus.2009.02.017.

Morgan, G.A., Head, J.W., Forget, F., Madeleine, J.-B., Spiga, A., 2010. Gully formation on Mars: Two recent phases of formation suggested by links between morphology, slope orientation and insolation history. Icarus. doi:10.1016/j.icarus.2009.02.017.

Morgenstern, A., Hauber, E., Reiss, D., van Gasselt, S., Grosse, G., Schirrmeister, L., 2007. Deposition and degradation of a volatile rich layer in Utopia Planitia and implications for climate history on Mars. J. Geophys. Res. 112. doi:10.1029/2006JE002869.

Mustard, J.F., Cooper, C.D., Rifkin, M.K., 2001. Evidence for recent climate change on Mars from the identification of youthful near-surface ground ice. Nature 412, 411–414.

Neukum, G., 10 colleagues, and the HRSC Co-Investigator Team, 2004. Recent and episodic volcanic and glacial activity on Mars revealed by the High Resolution Stereo Camera. Nature, 432, 971–979.

Peterson, J.E., 1977. Geologic Map of the Noachis Quadrangle of Mars. USGS, Misc. Geol., Inv. Map I-910.

Pierce, T.L., Crown, D.A., 2003. Morphologic and topographic analyses of debris aprons in the eastern Hellas region, Mars. Icarus 163, 46–65.

Plaut, J.J., Safaeinili, A., Holt, J.W., Phillips, R.J., Head, J.W., Seu, R., Putzig, N.E., Frigeri, A., 2009. Radar evidence for ice in lobate debris aprons in the mid-northern latitudes of Mars. Geophys. Res. Lett. 36, L02203. doi:10.1029/2008GL036379.

Reiss, D., Jaumann, R., 2004. Spring defrosting in the Russell Crater dune field—Recent surface runoff within the last martian year? Proc. Lunar Sci. Conf. 33. Abstract 2013.

Reiss, D., van Gasselt, S., Neukum, G., Jaumann, R., 2004. Absolute dune ages and implications for the time of formation of gullies in Nirgal Vallis, Mars. J. Geophys. Res. 109, E06007. doi:10.1029/2004JE002251.

Reiss, D., Hiesinger, H., Hauber, E., Gwinner, K., 2009. Regional differences in gully occurrence on Mars: A comparison between the Hale and Bond Craters. Planet. Space Sci. doi:10.1016/j.pss.2008.09.008.

Schon, S.C., Head, J.W., Fassett, C.I., 2009. Unique chronostratigraphic maker in depositional fan stratigraphy on Mars: Evidence for ~1.25 Ma old gully activity and surficial meltwater origin. Geology 37, 207–210. doi:10.1130/G25398A.25391.

Schultz, P.H., Glicken, H., 1979. Impact crater and basin control of igneous processes on Mars. J. Geophys. Res. 84, 8033–8047.

Schultz, P.H., Lutz, A.B., 1988. Polar wandering on Mars. Icarus 73, 91–141.

Scott, D.H., Carr, M.H., 1978. Geologic Map of Mars. U.S. Geol. Surv. Misc. Invest. Set., Map 1-1083, scale 1:25,000,000.

Shean, D.E., Marchant, D.R., 2010. Seismic and GPR surveys of Mullins Glacier, McMurdo Dry Valleys, Antarctica: Ice thickness, internal structure, and implications for surface ridge formation. J. Glaciol. 56 (195), 48–64.

Shean, D.E., Head, J.W., Marchant, D.R., 2005. Origin and evolution of a cold-based tropical mountain glacier on Mars: The Pavonis Mons fan-shaped deposit. J. Geophys. Res. 110, E05001. doi:10.1029/2004JE002360.

Shean, D.E., Head, J.W., Fastook, J.L., Marchant, D.R., 2007a. Recent glaciation at high elevations on Arsia Mons, Mars: Implications for the formation and evolution of large tropical mountain glaciers. J. Geophys. Res. 112, E03004. doi:10.1029/2006JE002761.

Shean, D.E., Head, J.W., Marchant, D.R., 2007b. Shallow seismic surveys and ice thickness estimates of the Mullins Valley debris-covered glacier, McMurdo Dry Valleys, Antarctica. Antarct. Sci. 19, 485–496. doi:10.1017/S0954102007000624.

Sizemore, H.G., Mellon, M.T., Searls, M.L., Lemmon, M.T., Zent, A.P., Heet, T.L., Arvidson, R.E., Blaney, D.L., Keller, H.U., 2010. In situ analysis of ice table depth variations in the vicinity of small rocks at the Phoenix landing site. J. Geophys. Res. 115, E00E09. doi:10.1029/2009JE003414.

Spry, A., 1962. The origin of columnar jointing, particularly in basalt flows. Geol. Soc. Aust. J. 8, 191–216.

Squyres, S.W., 1978. Martian fretted terrain: Flow of erosional debris. Icarus 34, 600–613.

Squyres, S.W., 1979. The distribution of lobate debris aprons and similar flows on Mars. J. Geophys. Res. 84, 8087–8096.

Sugden, D.E., Denton, G.H., Marchant, D.R., 1995. Landscape evolution of the Dry Valleys, Transantarctic Mountains: Tectonic implications. J. Geophys. Res. 100 (B7), 9949–9967.

Swanger, K.M., Marchant, D.R., Kowalewski, D.E., Head, J.W., 2010. Viscous flow lobes in central Taylor Valley, Antarctica: Origin as remnant buried glacier ice. Geomorphology. doi:10.1016/j.geomorph.2010.03.024.

Toramaru, A., Matsumoto, T., 2004. Columnar joint morphology and cooling rate: A starch–water mixture experiment. J. Geophys. Res. 109, B02205. doi:10.1029/2003JB002686.2004.02.

Védie, E., Costard, F., Font, M., Lagarde, J.L., 2008. Laboratory simulations of martian gullies on sand dunes. Geophys. Res. Lett. 35, L21501. doi:10.1029/2008GL035638.

Whalley, W.B., Azizi, F., 2003. Rock glaciers and protalus landforms: Analogous forms and ice sources on Earth and Mars. J. Geophys. Res. 108 (E4), 8032–8045.

Williams, R.M.E., Edgett, K.S., Malin, M.C., 2004a. Young fans in Equatorial Crater in Xanthe Terra, Mars. Lunar Planet. Sci. 35. Abstract 1415.

Williams, K.E., Toon, O.B., Heldmann, J.L., McKay, C., Mellon, M.T., 2008. Stability of mid-latitude snowpacks on Mars. Icarus 196, 565–577.

Williams, K.E., Toon, O.B., Heldmann, J.L., Mellon, M.T., 2009. Ancient melting of mid-latitude snowpacks on Mars as a water source for gullies. Icarus 200, 418–425. doi:10.1016/j.icarus.2008.12.013.